

# Synthesis and Biological Properties of Novel Pyridinioalkanoyl Thiolesters (PATE) as Anti-HIV-1 Agents That Target the Viral Nucleocapsid Protein Zinc Fingers

Jim A. Turpin,\*<sup>†,‡</sup> Yongsheng Song,<sup>§</sup> John K. Inman,<sup>‡</sup> Mingjun Huang,<sup>†,‡</sup> Anders Wallqvist,<sup>∇</sup> Andrew Maynard,<sup>∇</sup> David G. Covell,<sup>∇</sup> William G. Rice,<sup>†,||</sup> and Ettore Appella<sup>§</sup>

Laboratory of Antiviral Drug Mechanisms and Laboratory of Experimental and Computational Biology, National Cancer Institute—Frederick Cancer Research and Development Center, SAIC Frederick, P.O. Box B, Frederick, Maryland 21702-1201, Laboratory of Immunology, National Institute of Allergy and Infectious Diseases, National Institutes of Health, Bethesda, Maryland 20892-1892, and Laboratory of Cell Biology, National Cancer Institute, National Institutes of Health, Bethesda, Maryland 20892

Received April 24, 1998

Nucleocapsid p7 protein (NCp7) zinc finger domains of the human immunodeficiency virus type 1 (HIV-1) are being developed as antiviral targets due to their key roles in viral replication and their mutationally nonpermissive nature. On the basis of our experience with symmetrical disulfide benzamides (DIBAs; Rice et al. *Science* **1995**, 270, 1194–1197), we synthesized and evaluated variants of these dimers, including sets of 4,4'- and 3,3'-disubstituted diphenyl sulfones and their monomeric benzisothiazolone derivatives (BITA). BITAs generally exhibited diminished antiviral potency when compared to their disulfide precursors. Novel, monomeric structures were created by linking haloalkanoyl groups to the benzamide ring through –NH–C(=O)– (amide) or –S–C(=O)– (thiolester) bridges. Amide-linked compounds generally lacked antiviral activity, while haloalkanoyl thiolesters and non-halogen-bearing analogues frequently exhibited acceptable antiviral potency, thus establishing thiolester benzamides per se as a new anti-HIV chemotype. Pyridinioalkanoyl thiolesters (PATEs) exhibited superior anti-HIV-1 activity with minimal cellular toxicity and appreciable water solubility. PATEs were shown to preferentially target the NCp7 Zn finger when tested against other molecular targets, thus identifying thiolester benzamides, and PATEs in particular, as novel NCp7 Zn finger inhibitors for in vivo studies.

## Introduction

Successful applications of multidrug cocktails using inhibitors of HIV-1 protease and reverse transcriptase have been hailed as milestones in the treatment of AIDS. Unfortunately, combination therapy is negatively impacted by issues of patient compliance, drug toxicity, expense, the generation of multidrug-resistant phenotypes, and the presence of latent reservoirs of virus.<sup>1–3</sup> Moreover, damage to the immune system during HIV-1 infection prior to initiation of drug therapy can have profound effects on later immunocompetence. Thus, there exists a need for the development of agents that affect mutationally nonpermissive targets and which lack cross-resistance with current antiviral agents.

Nucleocapsid (NC) proteins of HIV-1 and all other retroviruses, except spumaretroviruses, contain one or two copies of a Cys (X)<sub>2</sub> Cys (X)<sub>4</sub> His (X)<sub>4</sub> Cys (CCHC) Zn finger motif.<sup>4–7</sup> The retroviral Zn finger motif is highly conserved. Mutations in either the conserved Zn chelating or nonchelating residues (both conserved and nonconserved) result in loss of NCp7-mediated activi-

ties, including rendering the virus noninfectious.<sup>8–12</sup> The dramatic findings from mutational studies on virus infectivity highlight the participation of the NCp7 protein in multiple activities during both early (reverse transcription<sup>13,14</sup> and integration<sup>15</sup>) and late (protease processing<sup>16</sup> and genomic RNA selection<sup>8</sup>) stages of HIV-1 replication. Thus, the NCp7 Zn finger motif offers a highly conserved target that is required for multiple stages of the virus replication cycle.<sup>17,18</sup>

Susceptibility of NCp7 Zn fingers to chemical modification was first demonstrated with 3-nitrosobenzamide (NOBA).<sup>19</sup> This finding was followed by the identification of a series of 2,2'-dithiobis(benzamide) disulfides (DIBA), which selectively targeted the HIV-1 NCp7 Zn fingers and were relatively nontoxic in vitro.<sup>20</sup> Select DIBAs inhibited a wide range of HIV-1 isolates whether expressed from acutely, latently, or chronically infected cells. In addition to other retroviruses (MuLV and SIV), DIBAs were also synergistic with AZT and other antiviral agents.<sup>20,21</sup> Mechanism of action studies in tumor necrosis factor alpha (TNF $\alpha$ )-induced latently infected U1 cells demonstrated that DIBA treatment resulted in extensive intracellular and intravirion cross-linkage of retroviral Zn finger-containing Gag precursors causing defects in protease processing,<sup>22</sup> whereas treatment of mature virions resulted in cross-linkage of mature NCp7 protein and prevention of initiation of reverse transcription.<sup>23</sup> More recently, DIBAs were found to selectively target NCp7 Zn fingers without affecting the

\* Corresponding author. Phone: (301) 694-3232. Fax: (301) 694-7223.

<sup>†</sup> Laboratory of Antiviral Drug Mechanisms.

<sup>‡</sup> Laboratory of Immunology.

<sup>§</sup> Laboratory of Cell Biology.

<sup>∇</sup> Laboratory of Experimental and Computational Biology.

<sup>†</sup> Present address: Southern Research Institute, 431 Aviation Way, Frederick, MD 21701-4756.

<sup>||</sup> Present address: Achillion Pharmaceuticals, 1003 West 7th St., Suite 401, Frederick, MD 21701.

functions of cellular Zn finger proteins such as poly-(ADP-ribose) polymerase and various transcription factors.<sup>24</sup> Further analysis of the interaction of DIBAs and other electrophilic chemotypes with the NCp7 Zn fingers using density-functional theory (DFT) in the context of the hard and soft acids and bases principle identified a significant correlation between rates of reaction and the ability of DIBAs to act as soft electrophiles.<sup>25</sup> Additionally, DFT calculations and molecular docking techniques identified the terminal cysteine (C49) of the second Zn finger as being the preferred site of reaction, in accord with the physical chemical studies of Hathout et al.<sup>26</sup>

Even though DIBAs represent a new class of highly specific antivirals, the disulfide bond is susceptible to reduction, affecting loss of activity. To circumvent this problem, two approaches have now been taken. The first involved substructure searches of chemical repositories for new antiviral chemotypes with Zn finger reactivity. Using this strategy, several new NCp7-reactive chemotypes have been identified, including dithianes and dithiolanes,<sup>27</sup> azo-containing compounds such as azodicarbonamide,<sup>28</sup> and additional disulfide-based chemotypes such as thiosulfones and thiosulfoxides.<sup>29</sup> The second approach, reported here, was to modify existing disulfide-based Zn finger-reactive chemotypes. Additionally, evidence that the monoliganded benzisothiazolones (BITA) have antiviral activity and the recent initiation of clinical trials in the United States with the BITA of DIBA-4<sup>20</sup> (now termed CI-1012) led us to concentrate our synthetic efforts on the DIBA and BITA chemotypes.<sup>30–32</sup>

We have divided the DIBA monomer into a reactive "head" group (sulfur-substituted benzamido) and "backbone" or "tail" group (benzenesulfonamide) based upon structural and physical evidence. Identification of an alternating hydrophilic–hydrophobic motif interaction that defined a cleft on the NCp7 surface led us to make extensions of the tail groups using readily available synthetic routes and intermediates.<sup>20,24,25</sup> Analogues of either DIBA-1 (**1**) or DIBA-2 (**2**) (and BITA monomers where synthetically feasible) with modified and extended tails were synthesized and analyzed for antiviral activity, cellular toxicity, and NCp7 Zn finger reactivity. Despite several promising analogues, the failure to generate new DIBA and BITA type compounds with substantially improved cytotoxicity, antiviral characteristics, and continued susceptibility to reduced glutathione led us to replace the S–S electrophilic moiety with other less reactive groups. Substituting a thiolester bridge for the disulfide led to the generation of a pyridinioalkanoyl thiolester (PATE) chemotype that possesses NCp7 Zn finger reactivity, virucidal activity, resistance to glutathione reduction, and appreciable aqueous solubility and also inhibits HIV-1 replication in both acutely and latently HIV-1-infected cells.

## Results

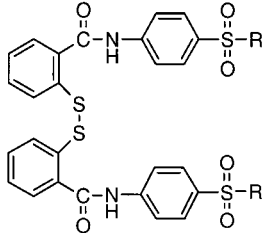
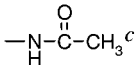
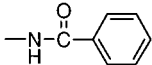
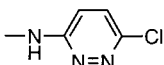
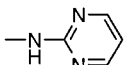
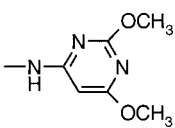
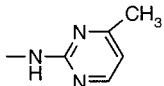
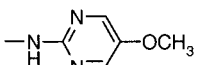
**Identification of Salient Interaction Features of the NCp7 Protein for Exploration of DIBA and BITA Chemotypes.** As a prelude to developing a pathway for the optimization of DIBA and BITA compounds we computationally scanned the solvent-accessible surfaces (SAS) of each Zn finger<sup>33</sup> for regions that

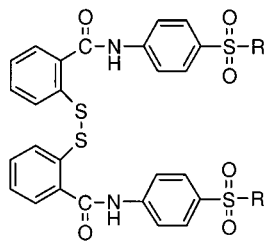
would favorably interact with a candidate ligand. The procedure for searching molecular surfaces is similar to that proposed by Goodford<sup>34</sup> but modified to include a larger range of atomic probes (manuscript in preparation) and a pairwise surface-based potential energy function to assess the free energy of interaction between the target and probe surfaces.<sup>35–37</sup> Analysis of the carboxy terminal Zn finger yielded a ligand prototype consisting of alternating hydrophilic and hydrophobic segments that could interact with the cleft formed by residues 38–43 and 47–51. The hydrophilic segments for the putative ligand are located at the ends and middle of the cleft, with intervening hydrophobic segments (i.e., Phil–Phob–Phil–Phob–Phil). The SAS of the Zn finger binding interface is 420 Å<sup>2</sup>, with approximately one-third of this surface comprising hydrophilic interactions with atoms C39:S<sup>γ</sup>, K41: N<sup>ε</sup>, G43:N, H44:N, N<sup>δ</sup>, M46:O, K47:O, D48:O, and E51:N. These atoms could participate in ligand-specific electrostatic interactions via hydrogen bonds and/or ion pairings. The remainder of the SAS involves hydrophobic interactions primarily with the aliphatic side chains of K38, K41, and E51 plus the C<sup>ε</sup> of H44 and the C<sup>β</sup>'s of C39 and C49. These hydrophobic patches account for two-thirds of the total SAS in this cleft. Together, these results suggest a minimal ligand design that would position alternating hydrophilic–hydrophobic groups in a linear arrangement. An ideally designed ligand, which resulted in optimal target interactions, would be predicted to have a moderate binding strength of ≈4.0 kcal/mol. Much of this interacting surface is formed by the Zn-coordinating residues C39, H44, and C49, which are completely conserved within the family of retroviral nucleocapsid Zn finger proteins. Residues G40, K41, and G43, which also are predicted to contribute strongly in ligand interactions, are also highly conserved. Analysis of the amino terminal finger yields a pattern similar to that of the carboxy terminal finger. These calculations provided a topography of the Zn finger surface interactions that was used as a conceptual guide for synthesis of DIBA and BITA analogues.

**Exploration of Disulfide Benzamide Phenylsulfonamido Ligand Structures.** In an effort to optimize antiviral activity, initial synthetic efforts were directed toward replacing ligand structures of compounds **1D** and **2D** (previously reported as DIBA-1 and DIBA-2, respectively<sup>20</sup>) with readily available synthetic intermediates. Disulfide (**D**) and where synthetically possible, the BITA (**B**), were synthesized to yield compounds **1B**, **2B**, and **3–22B** and **D** and **26D**, and their cellular toxicity and antiviral activity were assessed in the XTT cytoprotection assay (Tables 1–4). Among the new disulfide-based analogues produced, only compound **26D** (Table 3), created by converting the ligand portion of the DIBA into a bis(4-aminophenyl) sulfone, appeared promising. Compound **26D** exhibited no in vitro cellular toxicity at the high test concentration of 316 μM, exhibited an EC<sub>50</sub> (concentration inhibiting 50% virus replication) of 4.3 μM, and possessed moderate Zn finger reactivity. BITAs in general exhibited decreased antiviral efficacy with little or no modulation of cellular toxicity.

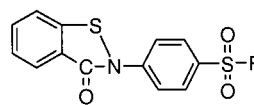
Additional synthetic efforts also addressed the efficacy of positional changes in the tail of DIBA-1 (**1**) by

**Table 1.** Synthesis of Novel Disulfides and Benzisothiazolone Forms Derived from the DIBA-1 and DIBA-2 Chemotypes

Compound	R	Form	Antiviral Activity <sup>a</sup>		
			EC <sub>50</sub> μM	IC <sub>50</sub> μM	TI
1.		D	0.85	217	255.3
		BITA	-	16.2	
2.		D	1.5	>200	>133
		BITA	12.6	34	2.7
3.		D	3.8	54.1	14.2
		BITA	9.3	49.5	5.3
4.		D	2.9	18.3	6.3
		BITA	7.1	19.2	2.7
5.		D	2	46.4	23.2
		BITA	6.5	50.8	7.8
6.		D	2.1	52.5	25
		BITA	7.6	56.6	7.4
7.		D	4.2	56.7	13.5
		BITA	8.8	57.4	6.5
8.		D	2.1	55.5	26.2
		BITA	17.8	57.6	3.3

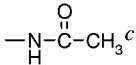
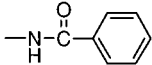
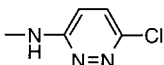
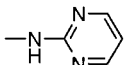
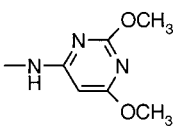
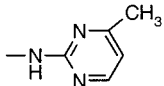
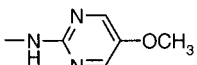


Dimer (D Form)



Benzisothiazolone (BITA Form)

Antiviral Activity<sup>a</sup>

Compound	R	Form	Antiviral Activity <sup>a</sup>		
			EC <sub>50</sub> μM	IC <sub>50</sub> μM	TI
1.	-NH <sub>2</sub> <sup>b</sup>	D	0.85	217	255.3
		BITA	-	16.2	
2.		D	1.5	>200	>133
		BITA	12.6	34	2.7
3.		D	3.8	54.1	14.2
		BITA	9.3	49.5	5.3
4.		D	2.9	18.3	6.3
		BITA	7.1	19.2	2.7
5.		D	2	46.4	23.2
		BITA	6.5	50.8	7.8
6.		D	2.1	52.5	25
		BITA	7.6	56.6	7.4
7.		D	4.2	56.7	13.5
		BITA	8.8	57.4	6.5
8.		D	2.1	55.5	26.2
		BITA	17.8	57.6	3.3

**Table 1** (Continued)

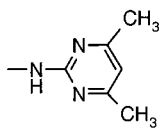
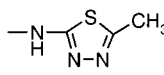
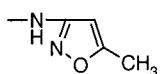
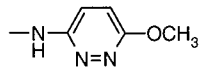
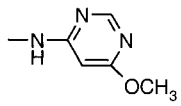
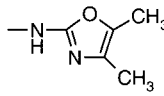
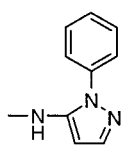
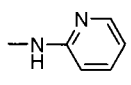
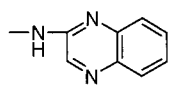
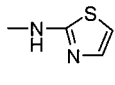
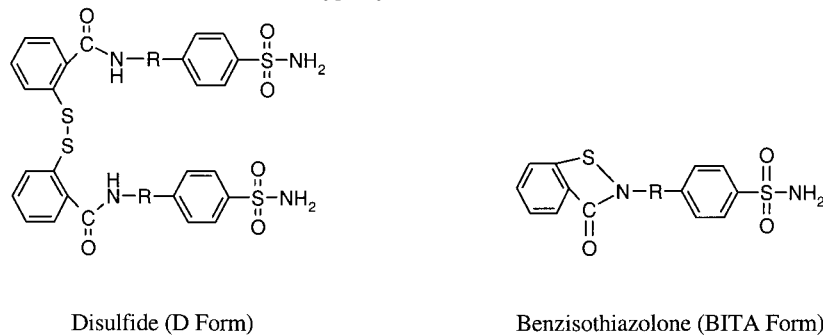
Compound	R	Form	Antiviral Activity <sup>a</sup>		
			EC <sub>50</sub> μM	IC <sub>50</sub> μM	TI
9.		D	1.6	32.2	20.1
		BITA	6.9	17.1	2.5
10.		D	3.4	18.6	5.5
		BITA	7.8	17.3	2.2
11.		D	1.9	27.6	14.5
		BITA	8.7	54.6	6.3
12.		D	4.2	53.8	12.8
		BITA	22.6	55.3	2.4
13.		D	1.6	46.5	29.1
		BITA	NT <sup>d</sup>		
14.		D	2.4	46.4	19.3
		BITA	NT		
15.		D	0.33	19.5	59.1
		BITA	NT		
16.		D	1.1	17.8	16.2
		BITA	NT		
17.		D	0.72	22.2	30.8
		BITA	9.2	54.7	5.9
18.		D	1	18	18
		BITA	NT		

Table 1 (Continued)

Compound	R	Form	Antiviral Activity <sup>a</sup>		
			EC <sub>50</sub> μM	IC <sub>50</sub> μM	TI
19.		D	1.9	18.2	9.6
		BITA	6.5	39.7	6.1
20.		D	2.5	44.2	17.7
		BITA	12.8	39.0	3.0
21.		D	111	>316	>2.8
		BITA	NT		
22.		D	2.3	43	18.7
		BITA	6.2	18.1	2.9

<sup>a</sup> Antiviral activity was measured in the XTT cytoprotection assay. <sup>b</sup> Originally reported as DIBA-1. <sup>c</sup> Originally reported as DIBA-2. <sup>d</sup> NT designates compounds that could not be made in sufficient quantity and/or purity to analyze.

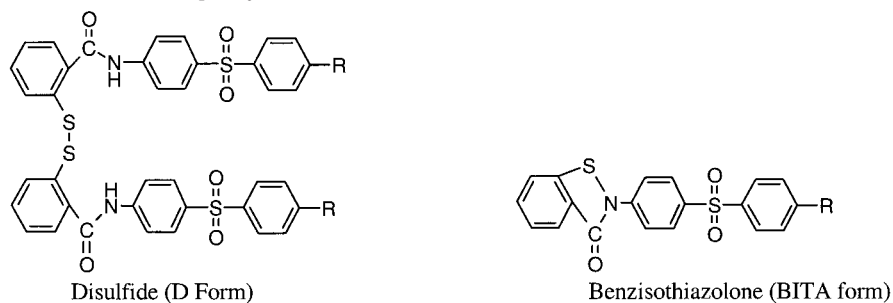
Table 2. Modification of the DIBA-2 Chemotype by Backbone Linker Substitutions



Compound	R	Form	Antiviral Activity <sup>a</sup>			Zinc Finger Reactivity RFU/ 30 min <sup>b</sup>
			EC <sub>50</sub> μM	IC <sub>50</sub> μM	TI	
23.	-CH <sub>2</sub> -	D	0.33	19.4	58.8	3.3
		BITA	13.8	53.7	3.9	2.7
24.	-(CH <sub>2</sub> ) <sub>2</sub> -	D	0.41	52.8	139	2.7
		BITA	2	45.5	22.7	2.7
25.		D	1.6	17.6	11	7.9

insertion of methylene or ethylene linkers prior to the benzenesulfonamide (Table 2, **23** and **24**). Antiviral activity was maintained, but these modifications were

associated with 4–10-fold more cytotoxicity when compared to the parental compound **1**. The corresponding BITAs again demonstrated a substantial loss of anti-

**Table 3.** Optimization of the Bis(aminophenyl) Sulfone-Based Disulfide Benzamides

Compound	R	Form	Antiviral Activity <sup>a</sup>			Zinc Finger Reactivity
			EC <sub>50</sub> μM	IC <sub>50</sub> μM	TI	RFU/min <sup>b</sup>
26.	-NH <sub>2</sub>	D	4.3	>316	>73.5	3.3
27.		D	1.5	160	106.7	5.9
28.		D	1.0	12.7	12.7	5.9
		BITA	9.6	188	19.6	7.9
29.		D	3.8	79.6	20.9	6.9
30.		D	12.2	190	15.6	-
31.	-NO <sub>2</sub>	D	12.2	>316	>26	2.9
		BITA	-	>316	-	4.1
32.		D	78	>316	>4	2.9
33.		D	240	>316	>1.3	1.6
34.		D	12.3	>316	>25.7	1.5
		BITA	3.2	59.5	15.1	2

ral activity (**23**, 42-fold and **24**, 5-fold decreases); however, Zn finger reactivity remained relatively constant. Further modification, by insertion of a glycol residue (**25**), enhanced Zn finger reactivity but did not result in a corresponding increase in antiviral activity.

**Exploration of Bis(aminophenyl) Sulfone-Based Disulfide Benzamides.** As noted above, incorporation

of 4,4'-bis(aminophenyl) sulfone into the disulfide backbone yielded **26D** with a terminal amine as a locus for further synthetic modifications. Acyl modifications of **26**, resulting in compounds **27–29** (Table 3) gave increased Zn finger reactivity and improved antiviral activity (decreased EC<sub>50</sub>). These gains were partially (**27** and **29**) and completely (**28**) offset by greater cytotoxicities.

**Table 4.** 3,3'-Bis(aminophenyl) Sulfone Isomers

Compound	R	Antiviral Activity <sup>a</sup>			Zinc Finger Reactivity
		EC <sub>50</sub> μM	IC <sub>50</sub> μM	TI	RFU/min <sup>b</sup>
35.	-NH <sub>2</sub>	1	81.5	81.5	0.92
36.		0.62	59.1	95	2

The BITA derivative of **26D** could not be produced in sufficient purity or quantity to study its properties. However, interchanging the terminal NH<sub>2</sub> of **26** for an NO<sub>2</sub> group (**31**) overcame this constraint and allowed for the production of both the disulfide and its corresponding BITA (Table 3). The disulfide form of **31**, like **26D**, was noncytotoxic, expressed equivalent NCp7 Zn finger reactivity, and exhibited moderate antiviral activity, even though it was less effective (**31**, EC<sub>50</sub> 12.2 μM vs **26**, EC<sub>50</sub> 4.3 μM). The BITA form of **31** was without antiviral activity. Exploration of ligand extensions with nitro aromatic groups led to compounds **32**–**34** of which only the disulfide of modification, **34**, had antiviral activity; Zn finger reactivity and lack of cytotoxicity were comparable to those of the simpler nitro forms (**31**).

Repositioning of the sulfonyl group to create 3,3'-bis-(aminophenyl) sulfones yielded isomers **35D** and **36D** (Table 4) with improved antiviral activities (**26D** vs **35D**, EC<sub>50</sub> 4.3 vs 1 μM; **27D** vs **36D**, EC<sub>50</sub> 1.5 vs 0.62 μM). These compounds exhibited greater cellular toxicity, thus providing no major advantages.

**Conversion of the Disulfide to a Thiolester.** Our failure to generate DIBAs or BITAs with substantially improved cytotoxicities and antiviral activities over the original DIBAs (**1** and **2**) prompted us to consider substituting a moderately active alkylating function in place of the disulfide group. Accordingly, using the DIBA-2 (**2**) backbone we synthesized monomer benzamides linked to haloalkanoyl groups via amide or thiolester bonds in either the ortho or meta benzamide positions (Table 5, **37**–**45**). Amide substitution via Cl-(CH<sub>2</sub>)<sub>2</sub>-CO-NH- in the ortho position generated compound **37**, which possessed low to moderate Zn finger reactivity and no antiviral activity. However, placing the Cl-(CH<sub>2</sub>)<sub>2</sub>-CO-NH- at the meta position (**38**) enhanced Zn finger activity and exhibited modest antiviral activity. Changing the ethylene spacer between the carbonyl and the halogen atom to a methylene group (**39**) in the ortho position abrogated Zn finger reactivity.

Thus, the failure of the amide linkage to promote satisfactory antiviral activity, even in the presence of good Zn finger reactivity, suggests that antiviral activity is determined by factors other than Zn finger reactivity, for this group of analogues, and identifies these compounds of interest only for NCp7 reactivity studies, not antiviral leads.

Alternatively using a thiolester linkage, we generated ortho-positioned, alkanoyl, aroyl, and haloalkanoyl thiolesters (**40**–**44**, Table 5). Synthesis of the acetyl (**40**), benzoyl (**41**), 4-methoxybenzoyl (**42**), and 3-chloropropionyl (**43**) thiolesters resulted in four compounds with low-micromolar EC<sub>50</sub> values and moderate to high Zn finger reactivity. However, cytotoxicities in the 50 μM range (equivalent to that of previously designed DIBAs and BITAs) diminished enthusiasm for these compounds, despite good Zn finger reactivity. Next, we modified the thiolester using ω-haloalkanoyl groups. The *o*-5-bromovaleroyl thiolester derivative of **2** (**44**) produced a compound with a 3-fold decrease in cytotoxicity that retained modest Zn finger reactivity and good antiviral activity (EC<sub>50</sub> 3.8 μM). Compound **44** was a substantial improvement over the other thiolesters, but aqueous solubility was a problem. In an attempt to reverse the solubility problem, the 5-bromovaleroyl thiolester was converted to a pyridiniovaleroyl thiolester (PATE, **45**). Compound **45** had improved solubility, (0.895 mg/mL), no cytotoxicity at the high test concentration of 316 μM, good antiviral activity, and Zn finger reactivity.

The initial success of the *o*-5-bromovaleroyl thiolester and pyridiniovaleroyl thiolester headgroups led us to generate similar modifications to compounds identified as either potential leads in earlier synthetic schemes (**27**, **31**, and **34**) or containing structural features of interest (**36** and **48**). Table 6 shows that PATE derivatives of these compounds consistently yielded analogues with equivalent or slightly improved cytotoxicity, antiviral activity, and Zn finger reactivity, compared to their parent disulfides. The activity profile of the PATE

**Table 5.** Single Liganded (Monomer) Benzamides Linked to Haloalkanoyl Groups via Amide or Thiolester Bonds

Compound	R1	R2	Antiviral Activity <sup>a</sup>			Zinc Finger Reactivity
			EC <sub>50</sub> μM	IC <sub>50</sub> %	TI	RFU/min <sup>b</sup>
<b>Amide:</b>						
37.		H	-	>316	-	2.0
38.	H		38	103	2.8	3.9
39.		H	-	202	-	0.3
<b>Thiolesters:</b>						
40.		H	2.8	56.7	20.3	4.2
41.		H	2.6	45.7	16.6	2.2
42.		H	2.8	43.7	15.6	3.5
43.		H	4.2	62	14.8	9.2
44.		H	3.8	184.5	49.2	1.8
45.		H	6.2	>316	>51	3.6

<sup>a</sup> Antiviral activity was measured by the XTT cytoprotection assay. <sup>b</sup> Zinc finger reactivity was measured by the Trp37 fluorescence assay. Results are expressed as the average decrease in relative fluorescence units over 30 min.

chemotype was also dependent on the length of the alkyl (**54** and **55**) spacer and required the thiolester link (compare with **56**, amide linker) to maintain low cell cytotoxicity and significant antiviral activity (Table 7). Together, this information indicates that the PATEs represent a new chemotype expressing a combination of favorable cytotoxicity, antiviral activity, and Zn finger reactivities.

**Antiviral Evaluation of Selected Pyridinioal-kanoyl Thiolesters.** Sufficient quantities of the 5-bromoaleroyl thiolester (**44**) and two 5-pyridinioaleroyl

thiolesters (**45** and **47**) were resynthesized at greater than 99% purity for further analyses in mechanistic and target-based assays. These compounds did not inhibit HIV-1 integrase, reverse transcriptase, protease, or virus attachment and fusion to host cells (Table 8). In contrast, all three compounds reacted with the NCp7 protein, as assessed by the Trp37 assay.

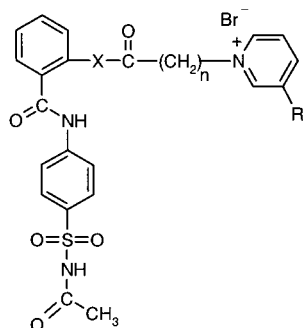
Interaction of Zn finger inhibitors with the NCp7 protein results in loss of Zn finger structure and the ability to specifically bind oligonucleotides containing the HIV-1  $\psi$  packaging site.<sup>24</sup> Figure 1A shows, using



**Table 6.** Evaluation of Pyridinioalkanoyl Thiolesters (PATEs) and 4-Bromovaleroyl Thiolesters

Compound	R Group	Antiviral Activity <sup>a</sup>			Zinc Finger Reactivity
		EC <sub>50</sub> % μM	IC <sub>50</sub> μM	TI	RFU/min <sup>b</sup>
<div style="display: flex; justify-content: space-around; align-items: center;"> <div style="text-align: center;"> <math display="block">\text{S}-\overset{\text{O}}{\parallel}{\text{C}}-(\text{CH}_2)_4-\text{Br}</math> <b>R1</b> </div> <div style="text-align: center;"> <math display="block">\text{S}-\overset{\text{O}}{\parallel}{\text{C}}-(\text{CH}_2)_4-\overset{+}{\text{N}}\langle\text{pyridine ring}\rangle</math> <b>R2</b> Br<sup>-</sup> </div> </div>					
<b>Compound 2 Backbone:</b>					
44.	R1	3.8	184.5	49.2	1.8
45.	R2	6.2	>316	>51	3.6
<b>Compound 31 Backbone:</b>					
46.	R1	1.6	21.7	13.6	1
47.	R2	5.5	>316	>57	4.1
<b>Compound 23 Backbone:</b>					
48.	R2	1.1	55	50	1.4
<b>Compound 34 Backbone:</b>					
49.	R1	-	>316	-	1.9
50.	R2	2.9	>316	>109	0.86
<b>Compound 27 Backbone:</b>					
51.	R2	4.6	288	63	1.7
<b>Compound 36 Backbone:</b>					
52.	R2	4.9	205	43	1.1
<b>Partial Structure (R2):</b>					
53.		-	>316		4

<sup>a</sup> Antiviral activity was measured by the XTT cytoprotection assay. <sup>b</sup> Zinc finger reactivity was measured by the Trp37 fluorescence assay. Results are expressed as the average decrease in relative fluorescence units over 30 min.

**Table 7.** Evaluation of Structural Features Comprising the Pyridinioalkanoyl Side Chain of the PATEs

Compound	X	n	R	Antiviral Activity <sup>a</sup>			Zinc Finger Reactivity
				EC <sub>50</sub> % $\mu$ M	IC <sub>50</sub> $\mu$ M	TI	RFU/min <sup>b</sup>
54	S	3	H	10.1	175	17.3	2.2
45 (parental PATE)	S	4	H	6.2	>316	>51	3.6
55	S	5	H	10.5	69.7	6.5	1.9
56	NH	4	H	-	>316	-	2.6
57	S	4	Cl	54	264	4.8	0.2

<sup>a</sup> Antiviral activity was measured by the XTT cytoprotection assay. <sup>b</sup> Zinc finger reactivity was measured by the Trp37 fluorescence assay. Results are expressed as the average decrease in relative fluorescence units over 30 min.

**Table 8.** Antiviral Mechanism of Action

Activity <sup>b</sup>	Compound (IC <sub>50</sub> $\mu$ M <sup>a</sup> )		
	<b>44</b>	<b>45</b>	<b>47</b>
integrase	NI <sup>c</sup>	NI	NI
reverse transcriptase			
rAdT	NI	NI	NI
rCdG	NI	NI	NI
protease	NI	NI	100
zinc finger reactivity <sup>d</sup>	1.8 (13.3%)	3.6 (34.7%)	4.1 (17.9%)
attachment	NI	NI	NI
fusion	>100	77	99

<sup>a</sup> IC<sub>50</sub>, concentration of compound inhibiting 50% of the indicated activity. <sup>b</sup> All positive controls for individual assays are as noted in the Experimental Section. <sup>c</sup> No inhibition (NI) at a high dose test of 100  $\mu$ M. <sup>d</sup> Expressed as decrease in relative fluorescence units over 30 min (RFU/min), with percent total decrease in fluorescence given in parentheses.

electrophoretic mobility shift assays (EMSA) on non-denaturing polyacrylamide gels, that compound **45** inhibited the formation of DNA/NCp7 complexes at 1  $\mu$ M, while **44** and **47** inhibited complex formation at 100  $\mu$ M. The specificity of the **44**, **45**, or **47** interaction with the NCp7 protein CCHC type Zn finger was assessed using a super shift EMSA to detect reactivity with the Sp1 transcription factor (DNA binding via interaction with three CCHH Zn fingers<sup>24</sup>). Figure 1B shows that the three compounds failed to alter the pattern of super shifting of Sp1 bound to its DNA target, indicating specificity for the CCHC retroviral Zn finger. Additionally, the three target compounds failed to alter HeLa nuclear extract-promoted *in vitro* transcription from a HIV-1 LTR template<sup>24</sup> (data not shown).

The interaction of Zn finger inhibitors with cell-free virus can result in modification of intravirion NCp7 protein and loss of infectivity. Virion-associated NCp7 proteins from cell-free HIV-1<sub>MN</sub> treated with **44**, **45**, or **47** were evaluated by nonreducing Western blotting

using HIV-1 NCp7-specific antibodies. The PATE compound **45** mediated extensive cross-linking of NCp7 [comparable to DIBA-1 (**1**)], whereas its haloalkanoyl thiolester precursor (**44**) was a very poor NCp7 cross-linking agent (Figure 2, left panel). Even though PATE **47** has antiviral activity equivalent to that of **45**, it was not an effective NCp7 cross-linker (Figure 2, right panel). In all cases loss of NCp7 and formation of large molecular aggregates in non-denaturing gels were reversible by reduction with 2-mercaptoethanol ( $\beta$ -ME), indicative of disulfide cross-linkage of adjacent NCp7 molecules (data not shown).

Loss of virus infectivity is a consequence of the modification NCp7 by either stable adduct formation or cross-linking. Cell-free HIV-1<sub>NL4-3</sub> was preincubated for 2 h with various concentrations of **44**, **45**, and **47**; residual compound was removed by centrifugation. Treated virions were incubated for 48 h with indicator cells, and  $\beta$ -galactosidase expression in MAGI-CCR-5 cells was measured at 48 h. Compounds **44** and **45** inactivated virus with IC<sub>50</sub> (concentration resulting in 50% virus inactivation) values of 12.3 and 13.2  $\mu$ M, respectively. Although **47** was not a potent cross-linker of intravirion NCp7 (see Figure 2, right panel), it was approximately 6-fold (IC<sub>50</sub> = 2.1  $\mu$ M) more potent than **44** and **45** at inactivating virus. These results suggest the formation of stable adducts with the Zn finger sulfur atoms which do not participate in the generation of inter- or intramolecular disulfide cross-linkages.

Table 6 shows that 5-pyridiniovaleric acid (**53**), in the absence of linkage to a monobenzamide tail, ejected Zn from the NCp7 protein (4 RFU/min), was noncytotoxic, but failed to express antiviral activity. Compound **53** was further assessed for intravirion cross-linking of NCp7 and virucidal activity to determine the relative contribution of this moiety to these activities in the

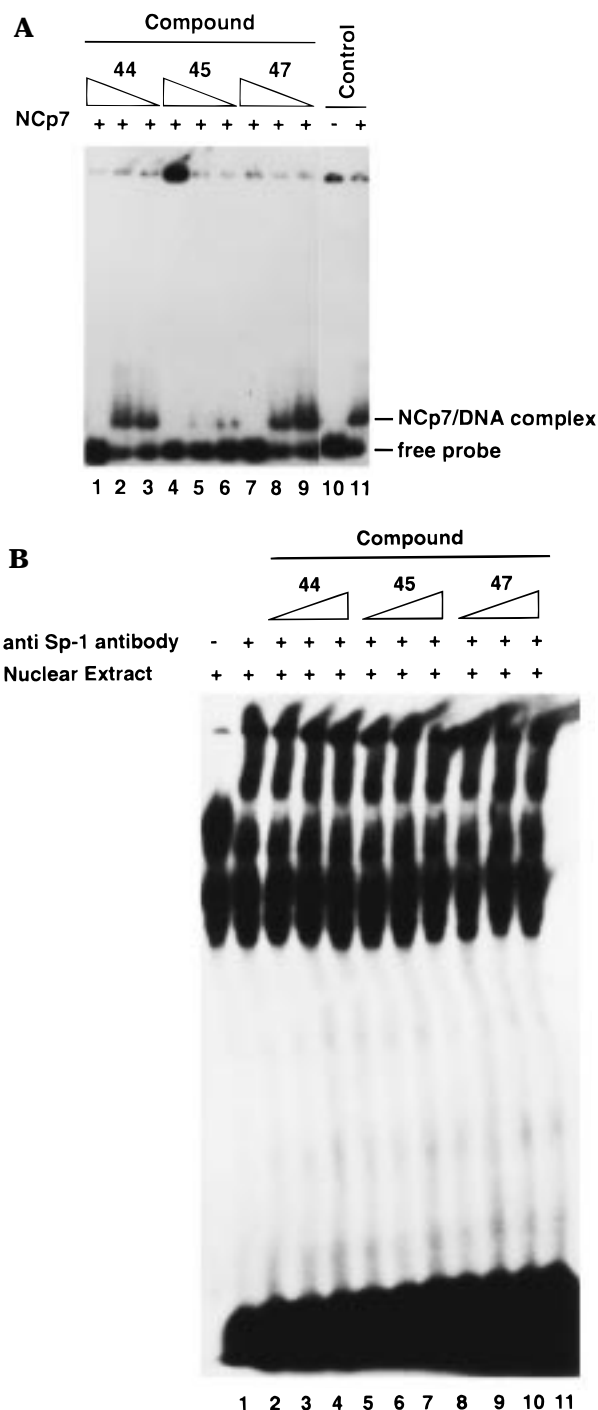


**Figure 1.** Effect of NCp7-reactive compounds on nucleoprotein complex formation. (A) Inhibition of nucleic acid–NCp7 complexes by zinc finger inhibitor compounds. Recombinant NCp7 was treated for 1 h with 100, 10, or 1  $\mu$ M **44**, **45**, and **47**. At the end of the treatment a  $^{32}$ P-labeled  $\psi$  site containing DNA oligomer was added, and protein nucleic acid complexes were separated by nondenaturing polyacrylamide gel electrophoresis. (B) Failure of **44**, **45**, and **47** to inhibit Sp1 transcription factor binding. K562 cell nuclear extracts were treated for 1 h with the indicated compounds at 1, 10, or 100  $\mu$ M and then annealed to the Sp1 target DNA sequence, with or without the addition of a super-shifting anti-Sp1 antibody.

PATEs. No intravirion cross-linkage of NCp7 (Figure 2, left panel) or virucidal activity (data not shown) was detected. Although the alkylpyridinio group may participate in the total Zn finger reactivity of PATEs, linkage to the monobenzamide tail is required for

realization of antiviral activity in acutely infected cells or cell-free virions.

Certain Zn finger-reactive compounds are potent inhibitors of HIV-1 replication in TNF $\alpha$ -induced, latently infected U1 cells due to their ability to modify intracellular HIV-1 precursor polyproteins containing the CCHC Zn finger motif.<sup>22</sup> U1 cells (Figure 3) were induced with 5 ng/mL TNF $\alpha$  in the presence of various concentrations of **44**, **45**, or **47**, and 48 h later p24 antigen expression and cell viability were determined by XTT dye reduction. All three compounds inhibited HIV-1 expression (p24) from U1 cells (EC<sub>50</sub>: 94.0, 42.2, and 10.7  $\mu$ M for **44**, **45**, and **47**, respectively), with no evidence of cellular cytotoxicity at a high test concentration of 300  $\mu$ M for **45** and **47** and 60% cytotoxicity at 200  $\mu$ M for **44** (data not shown). Inspection of viral proteins from TNF $\alpha$ -induced U1 cells by Western blotting revealed that **45** and **47** induced cross-linking of Zn finger-containing HIV-1 proteins, and reduction of the U1 protein preparations with  $\beta$ -ME showed that both **45** (100  $\mu$ M) and **47** (all doses) inhibited Pr55<sup>Gag</sup> (Gag) precursor processing in a manner similar to that reported for DIBA-1 (Figure 4B).<sup>22</sup> Compound **44** also cross-linked NCp7 and inhibited Gag precursor processing at an intermediate level between **45** and **47** (data not shown). Thus, PATEs initiate intracellular disulfide cross-linking of precursor polyproteins during late phase virus assembly and inactivate virus via an attack on the mature NCp7 retroviral Zn fingers in the cell-free virus.

In reducing environments the disulfide group of DIBAs becomes reduced to monomeric forms and mixed disulfides, with little or no antiviral activity or Zn finger reactivity. All three compounds (**44**, **45**, and **47**) retained the capacity to react with the cysteine thiols of the NCp7 Zn finger in the Trp 37 assay after a 2-h treatment with up to 8 molar excess of reduced glutathione, whereas compound **1** (DIBA-1) lost all Zn ejection capacity after exposure to a 2 molar excess of reduced glutathione. Thus, 5-bromovaleroyl (**44**) or 5-pyridiniovaleroyl (**45** and **47**) thioesters exhibit partial to complete resistance to reductive agents and subsequent loss of Zn finger reactivity.

**Molecular Modeling of PATE 45 onto the Retroviral Zn Finger.** Molecular docking was used to determine whether selected compounds could be positioned in the putative interaction cleft such that the reactive centers on the ligand and Zn finger target could favorably interact. This analysis attempts to identify possible conformations of a heretofore unobserved pre-reaction complex. In the absence of such data, information obtained from this analysis can provide a basis for interpreting reaction data and suggest alternative ligand designs. As an example PATE **45** is docked to the C-terminal Zn finger in Figure 5. This ligand geometry corresponds to the lowest energy conformation, obtained by iteratively sampling the minima of flexible rotamers, using CVFF force field Discover97.0 (MSI Inc., San Diego, CA). The final docked arrangement buries 508  $\text{\AA}^2$  of the Zn finger SAS. The ligand is positioned in the interaction cleft such that the thioester and pyridinium groups are located in a cleft formed by residues C39, K40, and K41 on one side and E51 on the opposite side. The  $-\text{SO}_2\text{NHCOCH}_3$  tail, at

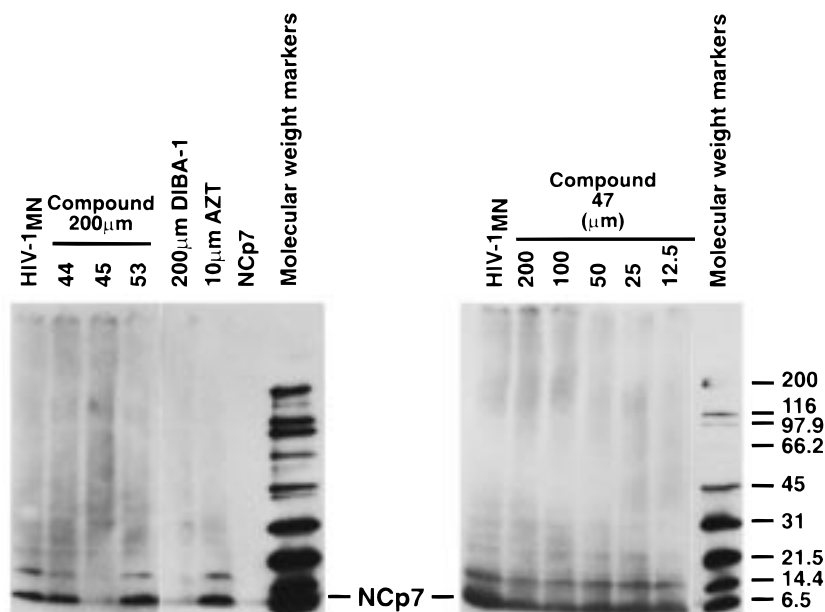


**Figure 2.** Intravirion cross-linking of NCp7 by selected PATEs. Purified HIV-1<sub>MN</sub> was incubated for 2 h with the indicated concentrations of **44**, **45**, **47**, **53**, DIBA-1<sup>29</sup> (**1**), or AZT. Following incubation, virus was concentrated and compound removed by centrifugation prior to Western blotting. Western blotting was performed using goat anti-NCp7 polyclonal antibody after resolution of the proteins on nonreducing 4–20% Tris-glycine polyacrylamide gels.

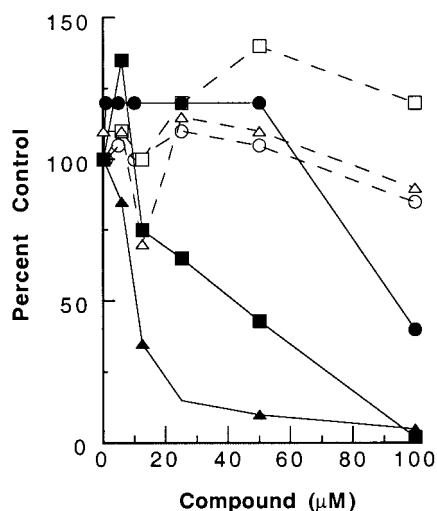


**Figure 3.** Inhibition of HIV-1 replication by selected PATEs in latently infected TNF $\alpha$ -induced U1 cells. U1 cells were simultaneously treated for 48 h with TNF $\alpha$  (5 ng/mL) and various concentrations of **44**, **45**, or **47**. At 48 h, cell-free supernatants were collected for p24 ELISA, and cellular viability was determined by XTT dye reduction: open symbols, cellular viability; closed symbols, supernatant p24; (○, ●) compound **44**; (□, ■) compound **45**; (△, ▲) compound **47**.

the opposite end of the molecule, is positioned in the pocket formed by residues M46–T50. The docking arrangement mimics the alternating Phil–Phob pattern described above that was observed during early stages of this project. The strongest contributions, toward the predicted binding strength of 3.2 kcal/mol, involve hydrophobic interactions between the ligand alkyl chain with the C, C $\alpha$ , C $\beta$ , and C $\gamma$  atoms of E51 (79 Å<sup>2</sup>), the phenyl rings with the C and C $\beta$  carbons of C39 (54 Å<sup>2</sup>), and the aliphatic side-chain carbons of K38 (72 Å<sup>2</sup>). These results indicate that the two phenyl rings of this compound, as well as the alkyl linker to the pyridinium group, participate in hydrophobic interactions with NCp7. All oxygen atoms, with the exception of the

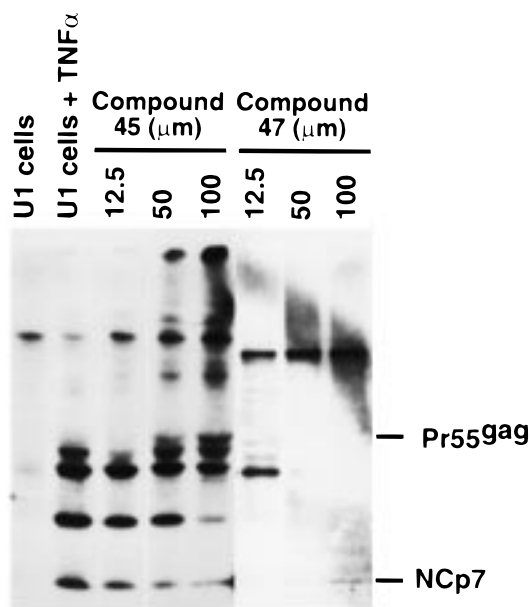
sulfonyl group, are positioned to make hydrogen bonds with residues K38, M46, C49, and E51. The thiolester is positioned 6 Å from the thiolate of S49 with the pyridinium ring oriented equidistantly (5 Å) from thiolates S39 and S49. This latter arrangement suggests a possible charge-transfer interaction with this electronegative region of the Zn finger. Thus, the mechanism by which PATE analogues chemically alter NCp7 may involve Zn finger oxidation by electron transfer or thiolate addition to the pyridinium ring via a charge-transfer intermediate.<sup>38</sup> These suppositions are being investigated by physicochemical measurements.

## Discussion

The involvement of HIV-1 NCp7 Zn fingers in multiple phases of the HIV-1 replication cycle and their mutationally nonpermissive nature have provided motivation for examining this structure as a target for antiretroviral therapy. We report the application of a multidiscipline approach to modify DIBAs and their corresponding BITA derivatives (where stable and synthetically possible) into new types of benzamido-linked ligands, and ultimately thiolester-based compounds. These efforts yielded monomeric pyridinioalkanoylester (PATE) derivatives that (1) target the CCHC Zn fingers of retroviral NC and Gag precursor proteins, (2) overcome the cellular toxicity associated with other nondisulfide-based forms, and (3) maintain Zn finger reactivity in the presence of reduced glutathione.

Molecular modeling of the NCp7 Zn fingers has identified ligand domains on the surface of both Zn fingers which allow for favorable ligand steric interactions and reactive accessibility to the nucleophilic Cys sulfurs. Molecular modeling has suggested that DIBAs were unique when compared with other known Zn finger inhibitors (azodicarbonamide,<sup>28</sup> 3-nitrosobenzamide,<sup>19</sup> and dithiane<sup>27</sup>), in that they could interact with two separate subdomains of a saddle-shaped binding

### A Non-reduced



### B Reduced

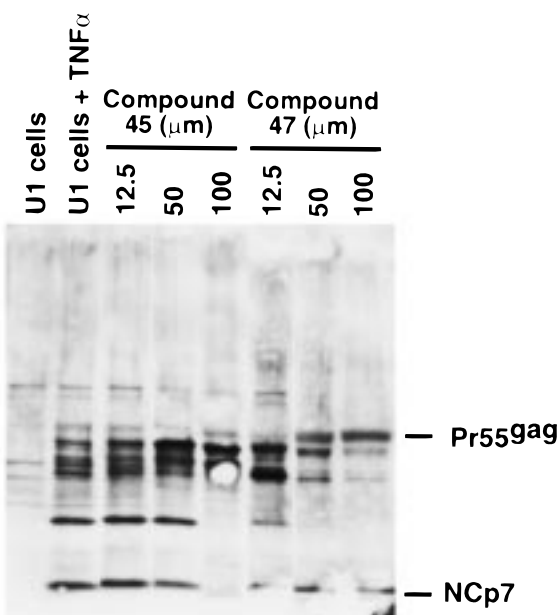


**Figure 4.** Inhibition of Gag precursor processing and cross-linking of Zn finger-containing HIV-1 precursor proteins in PATE-treated latently infected TNF $\alpha$ -induced U1 cells. U1 cells were treated simultaneously with various concentrations of **45** or **47** and 5 ng/mL TNF $\alpha$ . Forty-eight hours later, cellular proteins were harvested and resolved on 4–20% polyacrylamide gels under reducing or nonreducing conditions. Western blotting was visualized by chemiluminescence using a mixture of anti-NCp7 and anti-p24 antibodies: (A) nonreducing conditions, (B) reducing conditions.

cleft of NCp7.<sup>24</sup> Density functional theory (DFT) analysis suggested that the reactivity of NCp7 Zn finger is biased toward “soft” electrophiles.<sup>25</sup> In an effort to apply these observations to the development of improved DIBAs and BITAs, we identified the presence of an alternating hydrophilic–hydrophobic motif within the interaction cleft of both NCp7 Zn fingers as described above. Using this model and an approach utilizing

readily available synthetic intermediates, a number of DIBA and BITA analogues were synthesized by terminal modification of the benzenesulfonamide tail.

To facilitate the analysis of the new analogues, a gateway system was created which couples cell-based cytotoxicity and antiviral determinations (XTT cytoprotection assay) with a molecular target-based assay using purified recombinant NCp7 protein to measure Zn finger reactivity (Trp37 assay). Analogues exhibiting antiviral activity with 50% protection (EC<sub>50</sub>) values of  $\leq 10$   $\mu$ M, no cytotoxicity at the high test concentration of 316  $\mu$ M, and detectable Zn ejection were advanced for further study. Application of this gateway system to the newly synthesized compounds allowed identification and selection of analogues or synthetic pathways with favorable characteristics. However, disparities between the cell- and target-based assays were identified, suggesting that the employed modifications were not altering accessibility of the electrophile to the Zn fingers but rather modifying accessibility of the compound to its cellular or virion target. The Zn finger reactivity of compound **53** (5-pyridiniovaleric acid), in the absence of intravirion cross-linking of NCp7 and cell-based antiviral activity, illustrates this point by suggesting failure to penetrate viral or cellular membranes. These results suggest that efforts to develop effective Zn finger-reactive compounds for in vitro or in vivo inhibition of HIV-1 replication must concentrate on delivery and protection of the reactive species to the cell rather than on enhancing Zn finger reactivity in target-based assays.

Synthesis and analysis of new DIBA and BITA compounds (where stable and synthetically feasible) failed to identify specific leads with significantly improved antiviral, cell toxicity, or Zn finger reactivity profiles as compared to those of the parental DIBAs (**1** and **2**). However, tail extension did identify a series of compounds resulting from the conversion of the benzenesulfonamide to a bis(aminophenyl) sulfone or dapsone-like moiety. This series, typified by compounds **26**, **31**, and **34**, exhibited EC<sub>50</sub>'s in the 10  $\mu$ M range and mild Zn finger reactivity, while exhibiting no cytotoxicity at the high test concentration of 316  $\mu$ M. This finding contrasts with the properties of the parental compounds and the other tail extensions synthesized. Thus, the bis(aminophenyl) sulfone-containing analogues are a potential lead series for use in further synthetic modifications. In addition, we were able to characterize the relationship of the DIBAs and BITAs as to antiviral activity and cellular toxicity. Generally, conversion of the disulfide to a stable BITA form was associated with a loss of antiviral activity [average of a 4-fold ( $n = 15$ , range 1.5–8-fold) drop in the in vitro therapeutic index (IC<sub>50</sub>/EC<sub>50</sub>) due to increasing EC<sub>50</sub>] without significant changes in compound cytotoxicity. No overt generalizations were possible in regard to Zn finger activity for the DIBA and BITA pairs. Thus, our failure to identify a compound or series that possessed significant advantages in cytotoxicity, antiviral activity, Zn finger reactivity, or resistance to reduction over the parental DIBAs led us to explore other chemotypes bearing a monomeric structure.

Selecting the DIBA-2 (**2**) backbone as a template for modification, we generated monomeric forms using either amide or thiolester linkages with alkanoyl, aroyl,

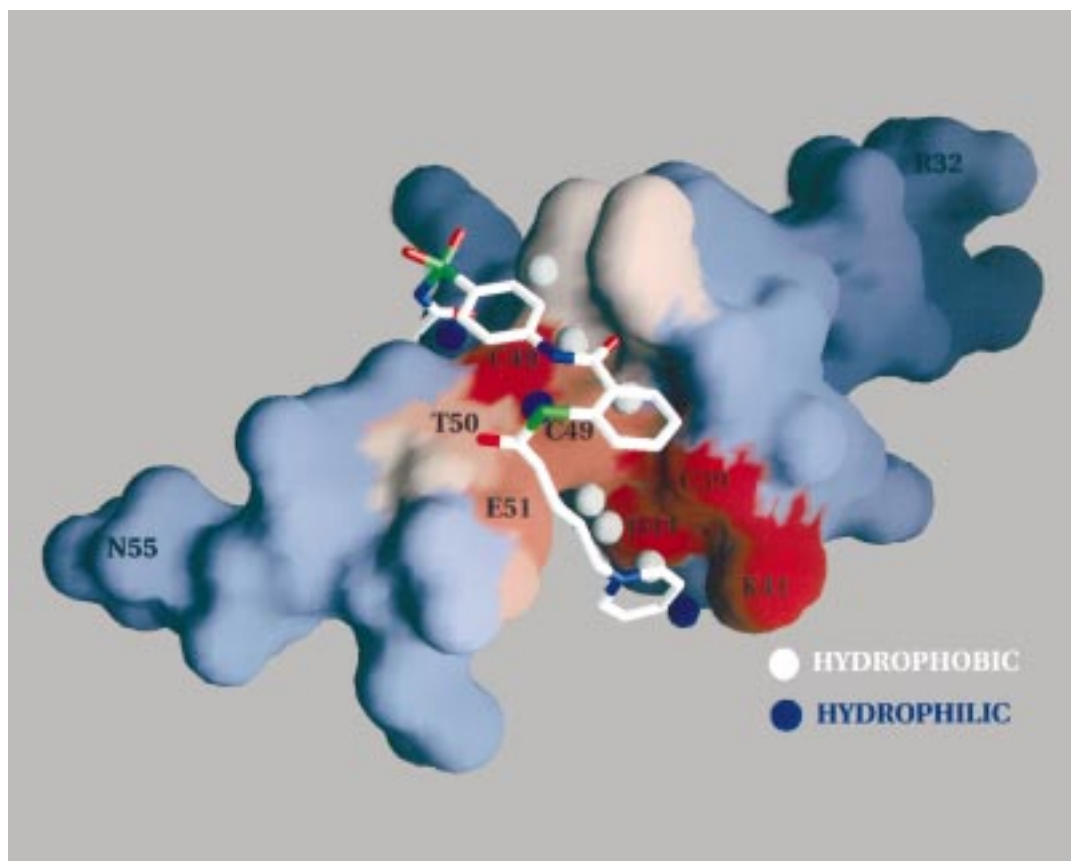


**Figure 5.** Solvent-accessible surface of the carboxy terminal NCp7 Zn finger. The regions of this surface predicted to have the strongest interactions with a candidate ligand are shaded in red; variations in the intensity of shading indicate regions with the greatest interaction strength (brightest) to regions of lowest interaction strength (pink). The set of optimal probe positions is displayed as small spheres. Probe positions specifying the location of hydrophobic and hydrophilic atoms are shown in gray and blue, respectively. These positions computationally identify the atom locations for an optimal ligand. The docked position of ligand **45** is displayed as a stick figure with carbon atoms shown in white, nitrogens in blue, oxygens in red, and sulfurs in green. The correspondence between ligand atoms and optimal probe positions finds that the correct ligand atom types are within van der Waals contact of their corresponding probe positions. Classification is based on sulfur, nitrogen, and oxygen atoms as hydrophilic atoms, with carbon as a hydrophobic atom type.

**Table 9.** Summary of Zinc Finger Reactivity for Compounds **44**, **45**, and **47**

Compound	NCp7 (Trp37)	Virion Cross-link	Nucleic Acid Binding (IC <sub>50</sub> μM)	Virucidal Activity (IC <sub>50</sub> μM)	U1 Cells	
					Inhibition of p24 (EC <sub>50</sub> μM)	Gag Precursor Cross-linking
<b>44</b>	+	-/+	100	12.3	94	+/-
<b>45</b>	+	+++	1	13.2	42.2	+/-
<b>47</b>	+	-/+	100	2.1	10.7	+++

and haloalkanoyl groups. These efforts generated a number of amides and thioesters with the following general characteristics (Table 5): (1) amides showed little or no antiviral activity (**37–39**) even if they possessed Zn finger reactivity, (2) all thioesters possessed some antiviral activity and Zn finger reactivity, and (3) the  $\omega$ -haloalkanoyl thioesters possessed the most favorable combination of antiviral and cytotoxicity properties [excluding the  $\omega$ -pyridinioalkanoyl thioesters (PATEs)] of the thioesters. Thus, the thioester function per se was identified as an active principle with favorable antiviral, cytotoxicity, and Zn finger-reactive characteristics. However, solubility problems associated with the  $\omega$ -haloalkanoyl thioesters presented challenges.

Subsequent synthesis of  $\omega$ -pyridinioalkanoyl thioesters from  $\omega$ -haloalkanoyl thioesters yielded compounds with improved solubility in aqueous buffers (giving solubilities of 0.895 and 0.625 mg/mL for **45** and **47**,

respectively, at room temperature in 0.5% NaHCO<sub>3</sub>, pH 7.5), decreased cellular toxicity, and resistance to glutathione reduction (Tables 6 and 7). An  $\omega$ -haloalkanoyl thioester (**44**) and two PATEs (**45** and **47**) were rigorously examined for their mode of action in mechanistic and target-based assays (Tables 8 and 9). Individually, these compounds were found to be active against the NCp7 Zn fingers whether presented in the context of cell or target-based assays, but not other antiviral molecular targets. The relative efficiencies of the three compounds in assays indicative of Zn finger reactivity are summarized in Table 9. As previously observed, antiviral activity as a result of Zn finger reactivity within a single chemotype can encompass compounds with different sites of action during HIV-1 replication.<sup>29</sup> Both compounds **45** and **47** were potent inhibitors of virus replication in the XTT cytoprotection assay and Zn ejectors in the Trp37 assay, but upon further

analysis these two PATEs demonstrated very different profiles of inhibition during the virus replication cycle. Compound **47** penetrates TNF $\alpha$ -induced U1 cells where it initiated precursor cross-linking and inhibition of Gag precursor processing. Interestingly, its potent activity against cell-free virions was not accompanied by extensive intravirion NCp7 cross-linkage. In contrast, action of compound **45** in cell-free virions was characterized by extensive intravirion cross-linkage of NCp7 and disruption of its ability to bind nucleic acids DNA. Interestingly, the precursor to **45** (**44**) lacking the pyridino group did not support cross-linkage of virion NCp7, yet **44** was a potent inactivator of cell-free virions, suggesting the formation of stable adducts.

Using a series of cell- and target-based assays measuring Zn finger reactivity, PATEs have been identified as Zn finger inhibitors. Supporting these biological evaluations, docking of **45** to the carboxy terminal Zn finger of the NCp7 protein suggests that it can theoretically occupy the described NCp7 interaction cleft, complementary to the alternating hydrophilic–hydrophobic motif. Furthermore, the pyridinium ring is located 5 Å from thiols S39 and S49 suggesting a charge-transfer interaction. Such an arrangement could promote oxidation of the Zn finger and possible thiolate addition to the pyridinium ring.<sup>38–40</sup> Studies have shown that nucleophilic addition can occur at ortho and para pyridinium positions.<sup>41,42</sup> Finally, DFT calculations have indicated that the softest electrophilic sites on the PATE **45** molecule correspond to these positions on the pyridinium ring (data not shown) and may account for the Zn finger activity associated with compound **53**. Interestingly, substitution of a chloro group in the meta position of the pyridinium ring (**57**) severely impaired antiviral activity and abrogated Zn finger reactivity, possibly due to an electrostatic interaction (repulsive) between the chloro group and residues S39 and S49. Analysis of the PATE reaction products is needed to resolve the reaction mechanism and is currently being pursued using NMR and mass spectrometric methods. The Zn finger reactivity of compounds **45** and **47** (monitored by decreases in Trp37 fluorescence over 30 min) may not represent the actual rate of Zn ejection due to quenching effects observed with these compounds. Finally, recent studies, using HPLC and mass spectrometry, indicate that both compounds indeed eject Zn<sup>2+</sup> and covalently modify NCp7 protein (manuscript in preparation).

Drug discovery efforts involving the participation of molecular modeling, medicinal chemistry, and antiviral assessment have led to the identification of the pyridinioalkanoyl thiolester (PATE) chemotype expressing antiviral activity by direct interaction with the NCp7 Zn fingers. This chemotype is currently being advanced for in vivo studies in animal models as a chemotherapeutic treatment for HIV-1 infection and as transmission preventatives (viral inactivation properties) with in vitro mucosal transmission models.

## Experimental Section

**Antiviral Evaluations. 1. Materials.** CEM-SS, MAGI-CCR-5, HL2/3, and U1 cells were obtained from the NIH AIDS Research and Reference Reagent Program (Bethesda, MD). CEM-SS and U1 cells were maintained in RPMI 1640, 10% FCS, 20  $\mu$ g/mL gentamicin, and 200 mM L-glutamate. MAGI-

CCR-5 cells were routinely passaged in selection media containing DMEM, 10% FCS, 20  $\mu$ g/mL gentamicin, 200 mM L-glutamate, 0.2 mg/mL G418, 0.1 mg/mL hygromycin B, and 1  $\mu$ g/mL puromycin. ELISA determinations of p24 in cell-free supernatants were done using kits purchased from the AIDS Vaccine Program (NCI–FCRDC, Frederick, MD). Recombinant, purified NCp7 for all assays was obtained using a pET3A-expressing NCp7 plasmid in *Escherichia coli*, strain BL21 (kind gift of R. De Guzman and M. F. Summers). Details for expression and purification of the NCp7 protein will be published elsewhere.

**2. Reference Reagents for Mechanistic and Target-Based Assays.** All positive control compounds for individual assays except AZTTP were obtained from the NCI chemical repository. The reference reagents for the individual assays are as follows: attachment, Farmatalia<sup>43</sup> (NSC 651016) and dextran sulfate (NSC 620255); reverse transcriptase inhibition, rAdT template/primer-AZTTP (Sierra BioResearch, Tuscon, AZ) and rCdG template/primer-UC38<sup>44</sup> (NSC 629243); protease inhibition, KNI-272<sup>45</sup> (NSC 651714); integrase inhibitor, ISIS 5320<sup>46</sup> (NSC 665353); fusion, Farmatalia<sup>43</sup> (NSC 651016) and dextran sulfate (NSC 620255); and NCp7 Zn<sup>2+</sup> ejection, virucidal activity, or virion cross-linking, dithiane<sup>27</sup> (NSC 624151) or DIBA-1<sup>20</sup> (NSC 654077).

**3. Antiviral Assay.** Antiviral activity of compounds was performed with CEM-SS cells and HIV-1<sub>RF</sub> (MOI = 0.01) using the XTT [2,3-bis(2-methoxy-4-nitro-5-sulfophenyl)-5-[(phenylamino)carbonyl]-2H-tetrazolium hydroxide] cytoprotection assay as previously described.<sup>19,27</sup> Effective antiviral concentrations providing 50% cytoprotection (EC<sub>50</sub>) and cellular growth inhibitory concentrations causing 50% cytotoxicity (IC<sub>50</sub>) were calculated. Efficacy of the compounds was further evaluated by calculation of the in vitro therapeutic index (IC<sub>50</sub>/EC<sub>50</sub>) which represents a relative measurement of antiviral success. 3'-Azido-2',3'-dideoxythymidine (AZT) and dextran sulfate were utilized as reference compounds for antiviral activity.

**4. U1 Assay.** Latently infected TNF $\alpha$ -inducible U1 cells were used to determine the effects of the compounds on late phase virus replication as previously described.<sup>22</sup> Briefly, U1 cells (5  $\times$  10<sup>4</sup> per 0.2-cm well) were simultaneously treated with 5 ng/mL TNF $\alpha$  and test compound. Cultures were continued for 48 h after which cell-free supernatants were collected for determination of p24 by the ELISA method. In selected experiments multiple wells were pooled, the cells were collected after centrifugation, and the resulting cell pellet was lysed in buffer containing 0.5% Triton X-100, 300 mM NaCl, 50 mM Tris-HCl, pH 7.5, 10  $\mu$ M leupeptin, 10  $\mu$ g/mL aprotinin, 1.8 mg/mL iodoacetamide, and 4 mM Pefabloc (Boehringer Mannheim, Indianapolis, IN) for Western blotting (described below).

**5. Zinc Finger Assays.** (1) Fluorescent measurements of the Trp37 residue in the C-terminal finger of recombinant HIV-1 NCp7 protein were performed as previously described.<sup>20,27</sup> Trp37 assays requiring pretreatment of the compound with reduced glutathione were carried out as follows. Two millimolars of compound was treated for 2 h at 37 °C with a 2–8 M excess of reduced glutathione; following incubation, the reactions were diluted 40-fold to a final concentration of 50  $\mu$ M compound, and Zn ejection was measured using the standard procedure. (2) Measurement of the ability of NCp7 to bind a DNA oligomer containing the HIV-1 RNA  $\psi$  packaging site (44 mer: GGC GAC TGG TGA GTA CGC CAA AAA TTT TGA CTA GCG GAG GCT AG) was carried out as previously described.<sup>24</sup> Briefly, 50 nM NCp7 was treated with test compounds for 1 h at room temperature in 10  $\mu$ L of buffer containing 10% glycerol and 50 mM Tris-HCl (pH 7.5). Labeled oligomer (0.1 pM, end labeled [<sup>32</sup>P]) was added in an equal volume of buffer containing 10% glycerol, 50 mM Tris-HCl (pH 7.5), 400 mM KCl, and 40 mM MgCl<sub>2</sub>. The reaction was continued for 15 min at room temperature, and a total of 5  $\mu$ L (or one-fourth of the total reaction volume) was separated on nondenaturing 4.5% polyacrylamide gels in 0.5X Tris-borate electrophoresis buffer. NCp7–oligomer complexes were visualized by autoradiography.

**6. Target-Based Assays.** Assays for activity against HIV-1 reverse transcriptase rAdT (template/primer) and rCdG (template/primer) using recombinant HIV-1 reverse transcriptase (a kind gift from S. Hughes, ABL Basic Research, NCI-FCRDC, Frederick, MD) have been previously described.<sup>27</sup> The substrate cleavage of recombinant HIV-1 protease in the presence of test compounds using an HPLC-based methodology with the artificial substrate Ala-Ser-Glu-Asn-Try-Pro-Ile-Val-amide (Multiple Peptide Systems, San Diego, CA) has been previously described.<sup>20,27</sup> The ability of recombinant HIV-1 integrase (a kind gift from S. Hughes, ABL Basic Research, NCI-FCRDC, Frederick, MD) to carry out 3'-processing and strand transfer activities in the presence of test compounds has been described.<sup>47,48</sup>

**7. Cell-Based Assays.** (1) The cell-based p24 attachment assay has been described in detail elsewhere.<sup>20</sup> (2) Viral inactivation assays were carried out as described with minor modifications.<sup>20,23</sup> Briefly, HIV-1<sub>NL4-3</sub> (obtained by transient transfection of HeLa cells with pNL4-3) was pretreated for 2 h at 37 °C after which residual compound was removed by centrifugation (18000g, 1 h, 4 °C). Virus pellets were resuspended, placed on 24-h old MAGI-CCR-5 (4 × 10<sup>4</sup> cells) monolayers, cultured for 48 h, fixed, and stained with X-Gal solution and blue cells counted. (3) Measurement of virus/cell fusion was carried out as follows. Briefly, HL2/3 cells stably expressing HIV-1 Tat and cell surface gp120 and MAGI-CCR-5 cells stably expressing CD4 and CCR5 on their cell surface, containing a β-galactosidase reporter gene under the control of the HIV-1 LTR, were pretreated with test compound for 1 h at 37 °C. After incubation, the cells were mixed in a 4:1 ratio [(2 × 10<sup>5</sup> MAGI-CCR-5 cells):(8 × 10<sup>5</sup> HL2/3 cells)] and cocultured for 18 h at 37 °C; cultures were fixed and stained with X-Gal solution for β-galactosidase activity. Blue cells represented the Tat transactivation of the HIV-1 LTR upon fusion of the HL2/3 and MAGI-CCR-5 cells via the CD4/CCR5 coreceptor gp120 interaction.

**8. Cross-Linking of NCp7 in Intact HIV-1 Virions.** Virion cross-linking was performed as previously described.<sup>20,23</sup> Briefly, HIV-1<sub>MN</sub> (11.8 μg of total protein) was incubated for 2 h at 37 °C with the indicated concentrations of compound. Virions were concentrated, and residual compound was removed by centrifugation (18000g, 1 h, 4 °C). The virus pellet was solubilized in 0.5 M Tris-HCl (pH 6.8), 50% glycerol, 8% SDS, and 0.4% bromophenol blue, and proteins were resolved by Western blotting (described below).

**9. Western Blotting.** Western blotting to detect the expression of HIV-1 proteins in U1 cells or virus pellets for virion cross-linking experiments was carried out as previously described.<sup>22</sup> Briefly, 50 μg of total cellular protein for U1 experiments or the total virion pellet for NCp7 cross-linking studies was resolved on 4–20% polyacrylamide gels in SDS with Tris-glycine (Novex, San Diego, CA). Samples for reduced gels were boiled for 5 min in the presence of 5% β-ME prior to loading. Resolved proteins were electroblotted on to poly(vinylidene difluoride) (PVDF) membranes, and HIV-1-specific proteins were detected using a mixture of goat anti-HIV-1 NCp7 and p24 or anti-NCp7 for virion proteins alone (a kind gift of L. E. Henderson, AIDS Vaccine Program, NCI-FCRDC, Frederick, MD). Western blots were developed using standard chemiluminescence methodologies (Dupont-NEN, Wilmington, DE).

**10. Transcription Factor Sp1 Super Gel Shifting.** Super gel shifting to determine the specificity of zinc finger-reactive compounds was carried out using an Sp1 consensus oligomer purchased from Stratagene (La Jolla, CA). K562 cell nuclear extracts and antibodies for Sp1 (Sp1[PEP2]-G) were obtained from Santa Cruz Biotechnology, Inc. (Santa Cruz, CA). The binding reactions of oligonucleotides with K562 nuclear extract as well as electrophoretic conditions were carried out as described in the Gelshift Buffer Kit (Stratagene, La Jolla, CA).

**Computational Modeling.** The NMR structure of NCp7,<sup>33</sup> obtained from the Protein Data Bank (PDB)<sup>49</sup> entry 1AAF, was treated as a rigid docking target. A previously published model of ligand binding<sup>35</sup> was used to analyze the interactions

between candidate reagents and the NCp7 protein. This model is based on the atomic preferences of adjacent surfaces buried at the binding interface and has been shown to accurately predict ligand binding strengths and assess the relative contributions of atomic interactions.<sup>36</sup> It has recently been extended to computational docking<sup>37</sup> and has proven effective for identifying ligands effective against NCp7<sup>29</sup> targets and providing testable hypotheses about the modes of action of candidate compounds to inhibit protein function.<sup>28</sup>

A variation of this model has been developed to scan the solvent-accessible surface of molecular targets to identify candidate binding sites (A. Maynard and D. Covell, manuscript in preparation). This procedure uses information about local geometry and chemical composition of subregions on the surface of NCp7 to select an atom type with optimal binding affinity at that site. The results of this procedure can be used to locate "hot spots" on the surface of the target ligand as well as suggest optimal atoms and their relative positions for a candidate ligand.

**Syntheses.** All organic reagents and intermediates were obtained from Sigma/Aldrich (St. Louis, MO) and Lancaster Synthesis, Inc. (Windham, NH). Solvents and others chemicals were reagent grade. Structure and composition of all compounds were verified by <sup>1</sup>H NMR and EI MS and analyzed by silica layer TLC, eluting with methanol/acetic acid (6:4) for pyridinioalkanoyl thiolester chemotype and chloroform/methanol (9:1) for the others. Representative syntheses are described below for each principal type of compound shown in Tables 1–7. Reaction pathways are illustrated in Schemes 1 and 2.

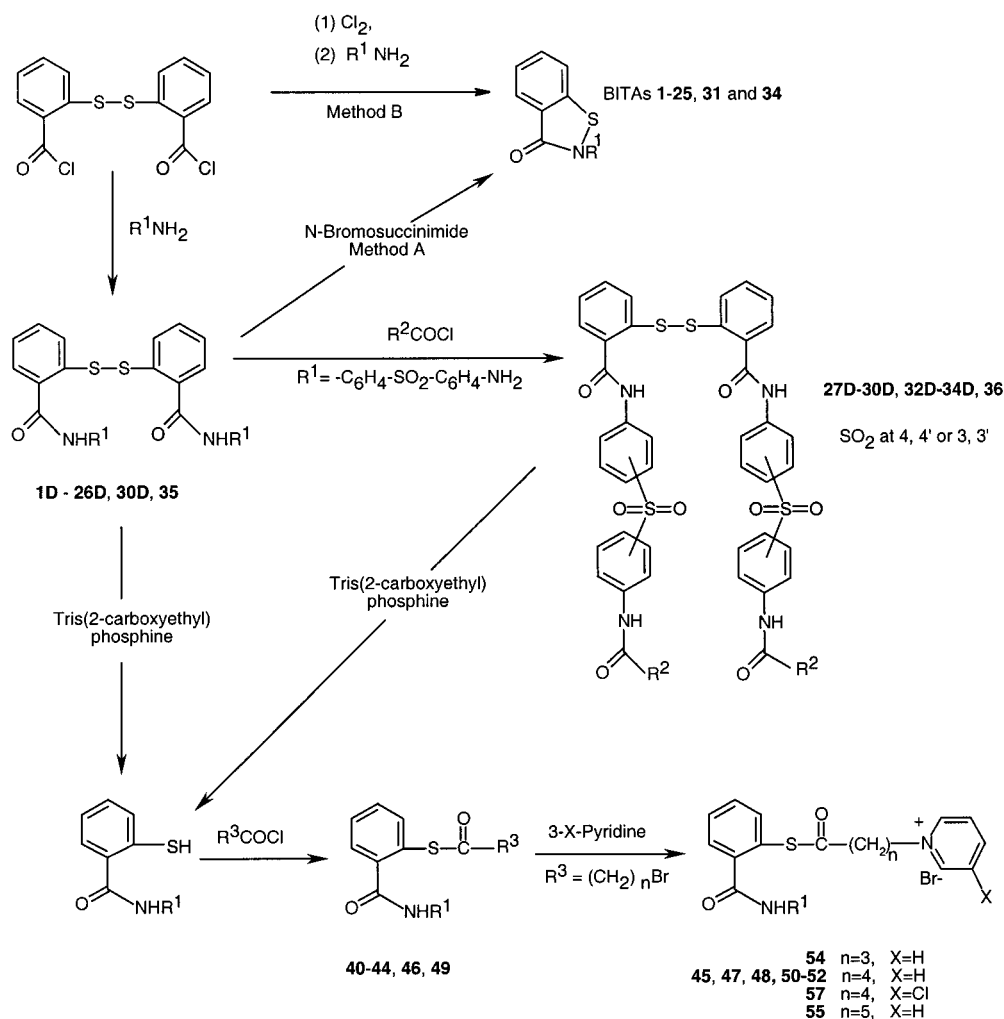
**Disulfide Benzamide Chemotype: 2D, *N,N*-(2,2'-Dithiodibenzoyl)bis(sulfacetamide).** The starting material, 2,2'-dithiodibenzoyl chloride, was synthesized as previously described.<sup>50,51</sup> To a solution of sulfacetamide (13 g, 60 mmol) in pyridine (300 mL) was added dropwise a solution of 2,2'-dithiodibenzoyl chloride (as 85%, 8.1 g, 20 mmol) in 1,4-dioxane (100 mL) at room temperature. The clear, reddish-brown solution was stirred at room temperature overnight and then poured into vigorously stirred ethyl ether (1 L). The viscous liquid precipitate was separated from the ether phase, dissolved in *N,N*-dimethylformamide (DMF; ~50 mL), and added dropwise to 800 mL of vigorously stirred, aqueous 3 M HCl. The white precipitate was filtered off, washed with water, and dried in a vacuum; yield, 11 g (78%). The crude product (1 g) was dissolved in hot ethanol (20 mL). The hot filtrate was added to stirred water (200 mL). The white precipitate was filtered off and dried: yield, 0.85 g (85%) of pure **2D**; mp = 257–260 °C dec; *R*<sub>f</sub> (CHCl<sub>3</sub>:MeOH, 9:1) = 0.10; <sup>1</sup>H NMR (DMSO-*d*<sub>6</sub>) δ 12.08 (s, 1H, HNSO<sub>2</sub>), 11.04 (s, 1H, HN-Ph), 8.01 (AB q, 4H, H-Ph), 7.87 (d, 1H, *J* = 7.6 Hz, H-Ph), 7.81 (d, 1H, *J* = 7.8 Hz, H-Ph), 7.59 (t, 1H, *J* = 7.7 Hz, H-Ph), 7.46 (t, 1H, *J* = 7.4 Hz, H-Ph), 1.97 (s, 3H, CH<sub>3</sub>); EI MS *m/z* 699 (MH<sup>+</sup>). Anal. (C<sub>30</sub>H<sub>26</sub>N<sub>4</sub>O<sub>8</sub>S<sub>4</sub>) C, H, N.

**Benzisothiazolone Chemotype: 2 BITA, *N*-[4-(3-Oxo-3*H*-benz[*d*]isothiazol-2-yl)phenylsulfonyl]acetamide.** **Method A:** To a solution of **2D** (0.2 g, 0.28 mmol) in pyridine (2 mL) was added a solution of *N*-bromosuccinimide (0.18 g, 1 mmol) in 1,4-dioxane (1 mL). The solution was stirred at room temperature for 3 h and added to water (30 mL). The white precipitate was collected and purified by precipitation from hot ethanol and water: yield, 0.17 g (87%); mp = 260–265 °C dec; *R*<sub>f</sub> (CHCl<sub>3</sub>:MeOH, 9:1) = 0.46; <sup>1</sup>H NMR (DMSO-*d*<sub>6</sub>) δ 12.24 (s, 1H, NH), 8.14 (d, 1H, *J* = 8.0 Hz, H-Ph), 8.10 (s, 4H, H-Ph), 8.02 (d, 1H, *J* = 7.8 Hz, H-Ph), 7.83 (t, 1H, *J* = 7.0 Hz, H-Ph), 7.56 (t, 1H, *J* = 7.6 Hz, H-Ph), 2.00 (s, 3H, CH<sub>3</sub>); EI MS *m/z* 349 (MH<sup>+</sup>). Anal. (C<sub>15</sub>H<sub>12</sub>N<sub>2</sub>O<sub>4</sub>S<sub>2</sub>) C, H, N.

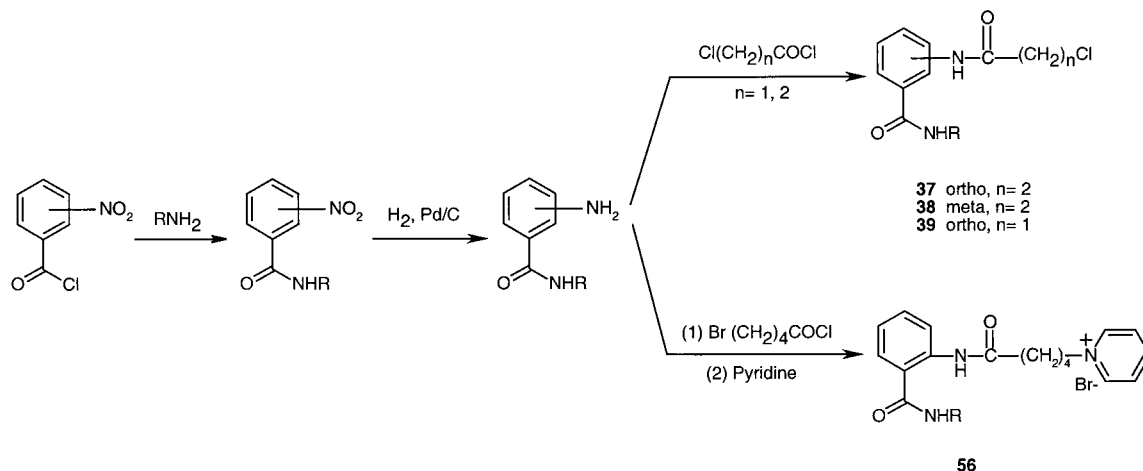
**Method B** (especially for **22 BITA**, **31 BITA**, and **34 BITA**): To a mixture of 2,2'-dithiodibenzoyl chloride (0.32 g, 0.93 mmol) in CCl<sub>4</sub> (10 mL) was added a solution of 2.5% w/v Cl<sub>2</sub> in CCl<sub>4</sub> (10 mL). The mixture was stirred until it cleared (1 h). After filtration, the filtrate was bubbled with N<sub>2</sub> for 1 h, and a solution of sulfacetamide (0.2 g, 0.93 mmol) in *N,N*-dimethylacetamide (DMA; 4 mL) was added. The mixture was stirred for 2 h, ethyl ether (20 mL) was added, and the precipitate was collected and purified with hot ethanol and



## Scheme 1



## Scheme 2



water: yield, 0.3 g (92%); mp = 250–254 °C dec; the same  $R_f$ ,  $^1\text{H}$  NMR, and EI MS as in method A. Anal. ( $\text{C}_{15}\text{H}_{12}\text{N}_2\text{O}_4\text{S}_2$ ) C, H, N.

**Spaced Disulfide Benzamide/Benzisothiazolone Chemotype:** **23D**, *N,N*-(2,2'-Dithiodibenzoyl)bis[4-(aminomethyl)benzenesulfonamide]; **24D**, *N,N*-(2,2'-Dithiodibenzoyl)bis[4-(2-aminoethyl)benzenesulfonamide]; **25D**, *N,N*-(2,2'-Dithiodibenzoyl)bis[4-(glycinamido)benzenesulfonamide]. These compounds were prepared, respectively, from 4-(aminomethyl)benzenesulfonamide (Aldrich), 4-(2-aminoethyl)benzenesulfonamide (Aldrich), and *N*-glycylsulfanil-

amide. The latter compound was prepared by first treating sulfanilamide with equimolar amounts of bromoacetyl bromide and pyridine in DMA and recovering the bromoacetylated derivative after adding the reaction mixture to excess 0.5 M HBr. The dried, crude product was recrystallized from ethanol and converted to *N*-glycylsulfanilamide via a standard Gabriel reaction (preparing the phthalimido derivative and cleaving with hydrazine hydrate). Procedures for **2D** were then followed.

**23D**: mp = 275–277 °C dec;  $R_f$  ( $\text{CHCl}_3:\text{MeOH}$ , 9:1) = 0.15;  $^1\text{H}$  NMR ( $\text{DMSO}-d_6$ )  $\delta$  9.34 (t, 1H,  $J = 6.1$  Hz, NH), 7.85 (d,

2H,  $J = 8.3$  Hz, H-Ph), 7.79 (d, 1H,  $J = 7.6$  Hz, H-Ph), 7.70 (d, 1H,  $J = 8.0$  Hz, H-Ph), 7.59 (d, 2H,  $J = 8.3$  Hz, H-Ph), 7.51 (t, 1H,  $J = 7.7$  Hz, H-Ph), 7.37 (m, 3H, NH<sub>2</sub> and H-Ph), 4.61 (d, 2H,  $J = 5.9$  Hz, CH<sub>2</sub>); EI MS  $m/z$  643 (MH<sup>+</sup>). Anal. (C<sub>28</sub>H<sub>26</sub>N<sub>4</sub>O<sub>6</sub>S<sub>4</sub>) C, H, N.

**24D**: mp = 270–272 °C;  $R_f$ (CHCl<sub>3</sub>:MeOH, 9:1) = 0.17; <sup>1</sup>H NMR (DMSO-*d*<sub>6</sub>) δ 8.81 (t, 1H,  $J = 5.2$  Hz, NH), 7.81 (d, 2H,  $J = 8.0$  Hz, H-Ph), 7.66 (d, 1H,  $J = 8.0$  Hz, H-Ph), 7.61 (d, 1H,  $J = 7.3$  Hz, H-Ph), 7.54–7.46 (m, 3H, H-Ph), 7.34 (m, 3H, NH<sub>2</sub> and H-Ph), 3.58 (q, 2H,  $J = 6.3$  Hz, CH<sub>2</sub>-N), 3.01 (t, 2H,  $J = 7.1$  Hz, CH<sub>2</sub>-Ph); EI MS  $m/z$  671 (MH<sup>+</sup>). Anal. (C<sub>30</sub>H<sub>30</sub>N<sub>4</sub>O<sub>6</sub>S<sub>4</sub>) C, H, N.

**25D**: mp = 273–274 °C dec;  $R_f$ (CHCl<sub>3</sub>:MeOH, 9:1) = 0.22; <sup>1</sup>H NMR (DMSO-*d*<sub>6</sub>) δ 10.53 (s, 1H, HN-Ph), 9.09 (t, 1H,  $J = 5.8$  Hz, HN-CH<sub>2</sub>), 7.87–7.83 (m, 5H, H-Ph), 7.72 (d, 1H,  $J = 7.1$ , H-Ph), 7.55 (t, 1H,  $J = 7.0$  Hz, H-Ph), 7.39 (t, 1H,  $J = 7.6$  Hz, H-Ph), 7.31 (s, 2H, NH<sub>2</sub>), 4.18 (d, 2H,  $J = 3.7$  Hz, CH<sub>2</sub>); EI MS  $m/z$  729 (MH<sup>+</sup>). Anal. (C<sub>30</sub>H<sub>28</sub>N<sub>6</sub>O<sub>8</sub>S<sub>4</sub>·H<sub>2</sub>O) C, H, N.

**N-Terminally Modified Aminophenyl Sulfone Chemotype: 34D, *N,N*-(2,2'-Dithiodibenzoyl)bis[4-sulfanyl-*N*-(2-nitrobenzoyl)sulfonyl]aniline**. Compound **26** was made in a similar manner as **2D**, starting with 4-aminophenyl sulfone and 2,2'-dithiodibenzoyl chloride. To a solution of **26** (1.5 g, 1.9 mmol) in DMA (30 mL) was added (dropwise) a solution of 2-nitro- $\alpha$ -toluenesulfonyl chloride (1.4 g, 5.9 mmol) in 1,4-dioxane (10 mL). The solution was stirred at room temperature overnight and then transferred to vigorously stirred ethyl ether (300 mL). After the ether phase was removed, the viscous liquid was diluted with DMF (15 mL). The diluted solution was added to water (200 mL) with stirring. The white precipitate was collected and purified by precipitation twice from hot ethanol and ethyl ether: yield, 1.92 g (84%); mp = 189–192 °C;  $R_f$ (CHCl<sub>3</sub>:MeOH, 9:1) = 0.34; <sup>1</sup>H NMR (DMSO-*d*<sub>6</sub>) δ 11.01 (s, 1H, HN-SO<sub>2</sub>), 10.74 (s, 1H, HN-CO), 8.10–7.29 (m, 16H, H-Ph), 5.11 (s, 2H, CH<sub>2</sub>); EI MS  $m/z$  1165 (MH<sup>+</sup>). Anal. (C<sub>52</sub>H<sub>40</sub>N<sub>6</sub>O<sub>14</sub>S<sub>6</sub>) C, H, N.

**2/3-Haloalkanoamido Benzamido Chemotype: 37, *N*-[2-(3-Chloropropionamido)benzoyl]sulfacetamide**. *N*-(2-Nitrobenzoyl)sulfacetamide was made in a similar manner as **2D**, but starting with 2-nitrobenzoyl chloride. One gram (2.7 mmol) of this product was dissolved in methanol (100 mL) at 45 °C. The solution was cooled to room temperature and then bubbled with N<sub>2</sub> to remove air. To the solution was added palladium, 10 wt % on activated carbon, (0.22 g) under N<sub>2</sub>. The mixture was bubbled with H<sub>2</sub> for 1.5 h and then with N<sub>2</sub> for 0.5 h. After filtration, the filtrate was evaporated to dryness; yield, 0.84 g (93%) of white-yellow product. This 2-aminobenzamido derivative was reacted with 3-chloropropionyl chloride under conditions similar to those described for **34D**, yielding **37**: mp = 220–222 °C dec;  $R_f$ (CHCl<sub>3</sub>:MeOH, 9:1) = 0.27; <sup>1</sup>H NMR (DMSO-*d*<sub>6</sub>) δ 12.06 (s, 1H, NH-SO<sub>2</sub>), 10.84 (s, 1H, NH-Ph), 10.32 (s, 1H, NH-Ph), 8.03–7.91 (m, 5H, H-Ph), 7.76 (d, 1H,  $J = 7.7$  Hz, H-Ph), 7.60 (t, 1H,  $J = 7.8$  Hz, H-Ph), 7.32 (t, 1H,  $J = 7.6$  Hz, H-Ph), 3.87 (t, 2H,  $J = 6.1$  Hz, CH<sub>2</sub>Cl), 2.86 (t, 2H,  $J = 6.2$  Hz, CH<sub>2</sub>), 2.00 (s, 3H, CH<sub>3</sub>); EI MS  $m/z$  424 (MH<sup>+</sup>). Anal. (C<sub>18</sub>H<sub>18</sub>N<sub>3</sub>O<sub>5</sub>SCl) C, H, N.

**Haloalkanoyl Thiolester Chemotype: 44, *N*-[2-(5-Bromovalerylthio)benzoyl]sulfacetamide**. *N*-(2-Mercapto-benzoyl)sulfacetamide was first prepared by adding to a solution of **2D** (2.2 g, 3.1 mmol) in 90% DMF (20 mL) tris(2-carboxyethyl)phosphine hydrochloride (1 g, 3.5 mmol) and triethylamine (0.5 mL). The solution was stirred for 1 h and then added to 0.5 M HCl (200 mL). The precipitate was collected and dried, yielding 2.3 g (95%). To a solution of this product (0.5 g, 1.4 mmol) in DMA (5 mL) was added 5-bromovaleryl chloride (0.6 mL, ~4.5 mmol) under N<sub>2</sub>. The solution was stirred under N<sub>2</sub> for 1 h and added to ethyl ether (50 mL). After the ether phase was decanted, the remaining viscous liquid was dissolved in DMF (10 mL). The solution was added to vigorously stirred water (100 mL). The white precipitate was filtered off and purified from hot ethanol and water: yield, 0.47 g (65%); mp = 190–195 °C dec;  $R_f$ (CHCl<sub>3</sub>:MeOH, 9:1) = 0.35; <sup>1</sup>H NMR (DMSO-*d*<sub>6</sub>) δ 12.05 (s, 1H, HNSO<sub>2</sub>), 10.91 (s,

1H, HN-Ph), 7.94 (s, 4H, H-Ph), 7.74–7.61 (m, 4H, H-Ph), 3.48 (t, 2H,  $J = 6.3$  Hz, CH<sub>2</sub>Br), 2.74 (t, 2H,  $J = 7.1$  Hz, CH<sub>2</sub>-CO), 1.96 (s, 3H, CH<sub>3</sub>), 1.90–1.64 (m, 4H, CH<sub>2</sub>CH<sub>2</sub>); EI MS  $m/z$  515 (MH<sup>+</sup>). Anal. (C<sub>20</sub>H<sub>21</sub>N<sub>2</sub>O<sub>2</sub>S<sub>2</sub>Br) C, H, N.

**Pyridinioalkanoyl Thiolester Chemotype: 45, *N*-[2-(5-Pyridiniovalerylthio)benzoyl]sulfacetamide Bromide**. A solution of **44** (0.25 g, 0.49 mmol) in pyridine (7 mL) was stirred under N<sub>2</sub> overnight. Ethyl ether (80 mL) was added, and the white precipitate was collected and purified from hot ethanol and ether; the precipitate was dried in a vacuum immediately: yield, 0.21 g (72%); mp = 193–195 °C;  $R_f$ (MeOH:AcOH, 6:4) = 0.45; <sup>1</sup>H NMR (DMSO-*d*<sub>6</sub>) δ 12.10 (br s, 1H, HNSO<sub>2</sub>), 10.94 (s, 1H, HN-Ph), 9.12 (d, 2H,  $J = 6.1$  Hz, 2,6-H-Py), 8.65 (t, 1H,  $J = 7.2$  Hz, 4-H-Py), 8.21 (t, 2H,  $J = 7.0$  Hz, 3,5-H-Py), 7.94 (s, 4H, H-Ph), 7.74–7.58 (m, 4H, H-Ph), 4.62 (t, 2H,  $J = 7.2$  Hz, CH<sub>2</sub>-Py), 2.79 (t, 2H,  $J = 7.2$  Hz, CH<sub>2</sub>-CO), 1.92 (m, 5H, CH<sub>3</sub> and CH<sub>2</sub>), 1.57 (pentet, 2H,  $J = 7.6$  Hz, CH<sub>2</sub>); EI MS  $m/z$  512 (M<sup>+</sup>). Anal. (C<sub>25</sub>H<sub>26</sub>N<sub>3</sub>O<sub>5</sub>S<sub>2</sub>Br) C, H, N.

**Acknowledgment.** This research was supported in part by the National Cancer Institute, Contract N01-Co-56000 (J.A.T., M.H., A.W., A.M., D.G.C., and W.G.R.), and by the Intramural AIDS Targeted Antiviral Program of the Office of the Director of the National Institutes of Health (E.A.). The content of this publication does not necessarily reflect the views or policies of the Department of Health and Human Services, nor does its mention of trade names, commercial products, or organizations imply endorsement by the U.S. government. We wish to thank Dr. Dennis Michaels (Monoclonal Antibody and Recombinant Protein Production Facility, NCI-FCRDC, Frederick, MD) for purification of NCp7 protein; Dr. Noel F. Whittaker for mass spectral analyses of compounds; Ms. Judy Dears for assistance in preparation of the manuscript; Ms. Terry Williams for preparation of figures; and Ms. Catherine Schaeffer, Lisa Graham, Carla Palamone, Karen Williamson, and Ming Bu for excellent technical assistance.

## References

- (1) Cohen, J. The daunting challenge of keeping HIV suppressed. *Science* **1997**, *277*, 32–33.
- (2) Wong, J. K.; Hezareh, M.; Günthard, H. F.; Havlir, D. V.; Ignacio, C. C.; Spina, C. A.; Richman, D. D. Recovery of replication-competent HIV despite prolonged suppression of plasma viremia. *Science* **1997**, *278*, 1291–1295.
- (3) Finzi, F.; Hermankova, M.; Pierson, T.; Carruth, L. M.; Buck, C.; Chaisson, R. E.; Quinn, T. C.; Chadwick, K.; Margolick, J.; Brookmeyer, R.; Gallant, J.; Markowitz, M.; Ho, D. D.; Richman, D. D.; Siliciano, R. F. Identification of a reservoir for HIV-1 in patients on highly active antiretroviral therapy. *Science* **1997**, *278*, 1295–1300.
- (4) Berg, J. M. Potential metal-binding domains in nucleic acid binding proteins. *Science* **1986**, *232*, 485–487.
- (5) Covey, S. N. Amino acid sequence homology in *gag* region of reverse transcribing elements and the coat protein gene of cauliflower mosaic virus. *Nucleic Acids Res.* **1986**, *14*, 623–633.
- (6) Green, L. M.; Berg, J. M. A retroviral Cys-Xaa<sub>2</sub>-Cys-Xaa<sub>4</sub>-His-Xaa<sub>4</sub>-Cys peptide binds metal ions: spectroscopic studies and a proposed three-dimensional structure. *Proc. Natl. Acad. Sci. U.S.A.* **1989**, *86*, 4047–4051.
- (7) Maurer, B.; Bannert, H.; Darai, G.; Flügel, R. M. Analysis of the primary structure of the long terminal repeat and the *gag* and *pol* gene of human Spumaretrovirus. *J. Virol.* **1988**, *62*, 1590–1597.
- (8) Aldovini, A.; Young, R. A. Mutations of RNA and protein sequences involved in human immunodeficiency virus type 1 packaging result in production of non infectious virus. *J. Virol.* **1990**, *64*, 1920–1926.
- (9) Méric, C.; Goff, S. P. Characterization of Moloney leukemia virus mutants with single-amino acid substitutions in the Cys-His box of the nucleocapsid protein. *J. Virol.* **1989**, *63*, 1558–1568.

- (10) Gorelick, R. J.; Chabot, D. J.; Ott, D. E.; Gagliardi, T. D.; Rein, A.; Henderson, L. E.; Arthur, L. O. Genetic analysis of the zinc finger in the Moloney leukemia virus nucleocapsid domain: replacement of zinc-coordinating residue with other zinc-coordinating residues yields noninfectious particles containing genomic RNA. *J. Virol.* **1996**, *70*, 2593–2597.
- (11) Dorfman, T.; Luban, J.; Goff, S. P.; Haseltine, W. A.; Göttlinger, H. G. Mapping of functionally important residues of a cysteine-histidine box in the human immunodeficiency virus type 1 nucleocapsid protein. *J. Virol.* **1993**, *67*, 6159–6169.
- (12) Kräusslich, H. G.; Fäcke, M.; Heuser, A.-M.; Konvalinka, J.; Zentgraf, H. The spacer peptide between human immunodeficiency virus capsid and nucleocapsid proteins is essential for ordered assembly and viral infectivity. *J. Virol.* **1995**, *69*, 3407–3419.
- (13) Darlix, J.-L.; Vincent, A.; Gabus, C.; De Rocquigny, H.; Roques, B. Trans-activation of the 5' to 3' viral DNA strand transfer by nucleocapsid protein during reverse transcription of HIV-1 RNA. *C. R. Acad. Sci. III* **1993**, *316*, 763–771.
- (14) Li, X.; Quan, Y.; Arts, E. J.; Preston, B. D.; De Rocquigny, H.; Roques, B. P.; Darlix, J.-L.; Kliemann, L.; Parniak, M. A.; Wainberg, M. A. Human immunodeficiency virus type 1 nucleocapsid protein (NCp7) directs specific initiation of minus-strand DNA synthesis primed by human tRNA<sub>3</sub><sup>Lys</sup> in vitro: studies of viral RNA molecules mutated in regions that flank the primer binding site. *J. Virol.* **1996**, *70*, 4996–5004.
- (15) Carteau, S.; Batson, S. C.; Poljak, L.; Mouscadet, J. F.; de Rocquigny, H.; Darlix, J. L.; Roques, B. P.; Kas, E.; Auclair, C. Human immunodeficiency virus type 1 nucleocapsid protein specifically stimulates Mg<sup>2+</sup>-dependent DNA integration in vitro. *J. Virol.* **1997**, *71*, 6225–6229.
- (16) Zybarth, G.; Carter, C. Domains upstream of the protease (PR) in human immunodeficiency virus type 1 Gag-Pol influence PR autoprocessing. *J. Virol.* **1995**, *69*, 3878–3884.
- (17) Gorelick, R. J.; Chabot, D. J.; Rein, A.; Henderson, L. E.; Arthur, L. O. The two zinc fingers in the human immunodeficiency virus type 1 nucleocapsid protein are not functionally equivalent. *J. Virol.* **1993**, *67*, 4027–4036.
- (18) Lapadat-Tapolsky, M.; De Rocquigny, H.; Van Gent, D.; Roques, B.; Plasterk, R.; Darlix, J.-L. Interactions between HIV-1 nucleocapsid protein and viral DNA may have important functions in the viral life cycle. *Nucleic Acid Res.* **1993**, *21*, 831–839.
- (19) Rice, W. G.; Schaeffer, C. A.; Graham, L.; Bu, M.; McDougal, J. S.; Orloff, S. L.; Villinger, F.; Young, M.; Oroszlan, S.; Fesen, M. R.; Pommier, Y.; Mendeleyev, J.; Kun, E. The site of action of 3-nitrosobenzamide on the infectivity process of human immunodeficiency virus in lymphocytes. *Proc. Natl. Acad. Sci. U.S.A.* **1993**, *90*, 9721–9724.
- (20) Rice, W. G.; Supko, J. G.; Malspeis, L.; Buckheit, R. W., Jr.; Clanton, D. J.; Bu, M.; Graham, L.; Schaeffer, C. A.; Turpin, J. A.; Domagala, J.; Gogliotti, R.; Bader, J. P.; Halliday, S. M.; Coren, L.; Sowder, R. C., II; Arthur, L. O.; Henderson, L. E. Inhibitors of HIV nucleocapsid protein zinc fingers as candidates for the treatment of AIDS. *Science* **1995**, *270*, 1194–1197.
- (21) Rein, A. D.; Ott, D. E.; Mirro, J.; Arthur, L. O.; Rice, W. G.; Henderson, L. E. Inactivation of murine leukemia virus by compounds that react with the zinc finger in the viral nucleocapsid protein. *J. Virol.* **1996**, *70*, 4966–4972.
- (22) Turpin, J. A.; Terpening, S. J.; Schaeffer, C. A.; Yu, G.; Glover, C. J.; Felsted, R. L.; Sausville, E. A.; Rice, W. G. Inhibitors of human immunodeficiency virus type 1 zinc fingers prevent normal processing of Gag precursors and result in the release of noninfectious virus particles. *J. Virol.* **1996**, *70*, 6180–6189.
- (23) Turpin, J. A.; Schaeffer, C. A.; Terpening, S. J.; Graham, L.; Bu, M.; Rice, W. G. Reverse transcription of human immunodeficiency virus type 1 is blocked by retroviral zinc finger inhibitors. *Antiviral Chem. Chemother.* **1997**, *8*, 60–69.
- (24) Huang, M.; Maynard, A.; Covell, D. G.; Janini, G. M.; Graham, L.; Turpin, J. A.; Rice, W. G. Anti-HIV-1 agents that selectively target retroviral nucleocapsid protein zinc fingers without affecting cellular zinc finger proteins. *J. Med. Chem.* **1998**, *41*, 1371–1381.
- (25) Maynard, A. T.; Huang, M.; Rice, W. G.; Covell, D. G. Reactivity of the HIV-1 nucleocapsid protein p7 zinc finger domains from the perspective of density-functional theory. *Proc. Natl. Acad. Sci. U.S.A.* **1998**, *95*, 11578–11583.
- (26) Hathout, Y.; Fabris, D.; Han, M. S.; Sowder, R. C., II; Henderson, L. E.; Fenselau, C. Characterization of intermediates in the oxidation of zinc fingers in human immunodeficiency virus type 1 nucleocapsid protein P7. *Drug Metab. Dispos.* **1997**, *24*, 1395–400.
- (27) Rice, W. G.; Baker, D.; Schaeffer, C. A.; Graham, L.; Bu, M.; Terpening, S.; Clanton, D.; Schultz, R.; Bader, J. P.; Buckheit, R. W., Jr.; Field, L.; Singh, P. K.; Turpin, J. A. Inhibition of multiple phases of HIV-1 replication by a dithiane compound that attacks the conserved zinc fingers of retroviral nucleocapsid proteins. *Antimicrob. Agents Chemother.* **1997**, *41*, 419–426.
- (28) Rice, W. G.; Turpin, J. A.; Huang, M.; Clanton, D.; Buckheit, R. W., Jr.; Covell, D. G.; Wallqvist, A.; McDonnell, N. B.; DeGuzman, R. N.; Summers, M. F.; Zalkow, L.; Bader, J. P.; Haugwitz, R. D.; Sausville, E. A. Azodicarbonamide inhibits HIV-1 replication by targeting the nucleocapsid protein. *Nature Med.* **1997**, *3*, 341–345.
- (29) Rice, W. G.; Turpin, J. A.; Schaeffer, C. A.; Graham, L.; Clanton, D.; Buckheit, R. W., Jr.; Zaharevitz, D.; Summers, M. F.; Wallqvist, A.; Covell, D. G. Evaluation of selected chemotypes in coupled cellular and molecular target-based screens identified novel HIV-1 zinc finger inhibitors. *J. Med. Chem.* **1996**, *39*, 3606–3616.
- (30) Tummino, P. J.; Harvey, P. J.; McQuade, T.; Domagala, J.; Gogliotti, R.; Sanchez, J.; Song, Y.; Hupe, D. The human immunodeficiency virus type 1 (HIV-1) nucleocapsid protein zinc ejection activity of disulfide benzamides and benzoisothiazolones: correlation with anti-HIV-1 and virucidal activities. *Antimicrob. Agents Chemother.* **1997**, *41*, 394–400.
- (31) Loo, J. A.; Holler, T. P.; Sanchez, J.; Gogliotti, R.; Maloney, L.; Reily, M. D. Biophysical characterization of zinc ejection from HIV nucleocapsid protein by anti-HIV 2,2'-dithiobis[benzamides] and benzoisothiazolones. *J. Med. Chem.* **1996**, *39*, 4313–4320.
- (32) Domagala, J. M.; Bader, J. P.; Gogliotti, R. D.; Sanchez, J. P.; Stier, M. A.; Song, Y.; Prasad, J. V. N. V.; Tummino, P. J.; Scholten, J.; Harvey, P.; Holler, T.; Gracheck, S.; Hupe, D.; Rice, W. G.; Schultz, R. A new class of anti-HIV-1 agents targeted toward the nucleocapsid protein NCp7: the 2,2'-dithiobisbenzamides. *Bioorg. Med. Chem.* **1997**, *5*, 569–579.
- (33) Summers, M. F.; Henderson, L. E.; Chance, M. R.; Bess, J. W., Jr.; South, T. L.; Blake, P. R.; Sagi, I.; Perez-Alvarado, G.; Sowder, R. C., III; Hare, D. R.; Arthur, L. O. Nucleocapsid zinc fingers detected in retroviruses: EXAFS studies on intact viruses and the solution-state structure of the nucleocapsid protein from HIV-1. *Protein Sci.* **1992**, *1*, 563–576.
- (34) Goodford, P. J. A computational procedure for determining energetically favorable binding sites on biologically important macromolecules. *J. Med. Chem.* **1985**, *28*, 849–857.
- (35) Wallqvist, A.; Jernigan, R. L.; Covell, D. G. A preference-based free-energy parametrization of enzyme–inhibitor binding: applications to HIV-1 protease inhibitor design. *Protein Sci.* **1995**, *4*, 1881–1903.
- (36) Covell, D. G.; Jernigan, R. L.; Wallqvist, A. Structural analysis of inhibitor binding to HIV-1 protease: identification of a common binding motif. *THEOCHEM* **1998**, *423*, 93–100.
- (37) Wallqvist, A.; Covell, D. G. Docking enzyme–inhibitor complexes using a preference based free-energy surface. *Proteins* **1996**, *25*, 403–419.
- (38) Kosower, E. M. *Molecular Biochemistry*; McGraw-Hill: New York, 1962; pp 166–219.
- (39) van Eys, J.; Kaplan, N. The addition of sulfhydryl compounds to the diphosphopyridine nucleotide and its analogues. *J. Biol. Chem.* **1957**, *228*, 305–314.
- (40) Katritsky, A.; Chen, J.; Wittman, D.; Marson, C. Formation of sigma and pi or charge-transfer complexes from pyridinium cations. *J. Org. Chem.* **1986**, *51*, 2481–2485.
- (41) Mendez, F.; Gazquez. The Fukui function of an atom in a molecule: a criterion to characterize the reactive sites of chemical species. *Proc. Ind. Acad. Sci.* **1994**, *106*, 183–193.
- (42) Doddi, G.; Ercolani, G.; Mencarelli, P. The problem of regioselectivity in nucleophilic additions to pyridinium and related cations: role of generalized anomeric effect. *J. Org. Chem.* **1992**, *57*, 4431–4434.
- (43) Clanton, D. J.; Buckheit, R. W., Jr.; Terpening, S. J.; Kiser, R.; Mongelli, N.; Borgia, A. L.; Schultz, R.; Narayanan, V.; Bader, J. P.; Rice, W. G. Novel sulfonated and phosphonated analogues of distamycin which inhibit the replication of HIV. *Antiviral Res.* **1995**, *27*, 335–354.
- (44) Bader, J. P.; McMahon, J. B.; Schultz, R. J.; Narayanan, V. L.; Pierce, J. B.; Harrison, W. A.; Weislow, O. S.; Midelfort, C. F.; Stinson, S. F.; Boyd, M. R. Oxathiin carboxanilide, a potent inhibitor of human immunodeficiency virus reproduction. *Proc. Natl. Acad. Sci. U.S.A.* **1991**, *88*, 6740–6744.
- (45) Kageyama, S.; Mimoto, T.; Murakawa, Y.; Nomizu, M.; Ford, H., Jr.; Shirasaka, T.; Gulnik, S.; Erickson, J.; Takada, K.; Hayashi, H.; Broder, S.; Kiso, Y.; Mitsuya, H. In vitro anti-human immunodeficiency virus (HIV) activities of transition state mimetic HIV protease inhibitors containing allophenyl-norstatine. *Antimicrob. Agents Chemother.* **1993**, *37*, 810–817.
- (46) Buckheit, R. W., Jr.; Roberson, J. L.; Lackman-Smith, C.; Wyatt, J. R.; Vickers, T. A.; Ecker, D. J. Potent and specific inhibition of HIV envelope-mediated cell fusion and virus binding by G quartet-forming oligonucleotide (ISIS 5320). *AIDS Res. Hum. Retroviruses* **1994**, *10*, 1497–1506.
- (47) Turpin, J. A.; Buckheit, R. W., Jr.; Darse, D.; Hollingshead, M.; Williamson, K.; Palamone, C.; Osterling, M. C.; Hill, S. A.; Graham, L.; Schaeffer, C. A.; Bu, M.; Huang, M.; Cholody, W. M.; Michejda, M. J.; Rice, W. G. Inhibition of acute-, latent-, and

- chronic-phase human immunodeficiency virus type 1 (HIV-1) replication by a bistriazoloacridone analogue that selectively inhibits HIV-1 transcription. *Antimicrob. Agents Chemother.* **1998**, *42*, 487–494.
- (48) Bushman, F. D.; Craigie, R. Activities of human immunodeficiency virus (HIV) integration protein in vitro; specific cleavage and integration of HIV DNA. *Proc. Natl. Acad. Sci. U.S.A.* **1991**, *88*, 1339–1343.
- (49) Bernstein, F. C.; Koetzle, T. F.; Williams, G. J. B.; Meyer, E. F., Jr.; Brice, M. D.; Rogers, J. R.; Kennard, O.; Shimanouchi, T.; Tasumi, M. The Protein Data Bank: a computer based archival file for macromolecular structures. *J. Mol. Biol.* **1977**, *112*, 535–542.
- (50) Katz, L.; Karger, L. S.; Schroeder, W.; Cohen, M. S. Hydrazine derivatives. I. Benzalthio- and bisbenzaldithio-salicylhydrazides. *J. Org. Chem.* **1953**, *18*, 1380–1402.
- (51) Baggaley, K. H.; English, P. D.; Jennings, L. J. A.; Morgan, B.; Nunn, B.; Tyrrell, A. W. R. Inhibitors of blood platelet aggregation. Effects of some 1,2-benzisothiazol-3-ones on platelet responsiveness to adenosine diphosphate and collagen. *J. Med. Chem.* **1985**, *28*, 1661–1667.

JM9802517